Combination of CP/MAS NMR and X-ray Crystallography: Structure and Dynamics in a Low-Symmetry Molecular Crystal, Potassium Penicillin V

Jamila Fattah,[†] J. Mark Twyman,[†,‡] Stephen J. Heyes,*[,†] David J. Watkin,[§] Alison J. Edwards,[§] Keith Prout,*[,§] and Christopher M. Dobson*[,†]

Contribution from the Inorganic Chemistry Laboratory, South Parks Road, Oxford OX1 3QR, U.K., and Chemical Crystallography Laboratory, 9 Parks Road, Oxford OX1 3PD, U.K.

Received November 2, 1992

Abstract: The variable-temperature ^{13}C CP/MAS NMR spectra of the potassium salt of phenoxymethylpenicillin ($C_{16}H_{17}N_2O_5SK$) (potassium penicillin V) at $T < 352$ K indicate an unusual low-symmetry structure with four molecules in the crystallographic asymmetric unit. This is confirmed by a single-crystal X-ray diffraction study, which employed a novel computational protocol to allow solution of the structure, which indicates that the four distinct molecules differ principally in the orientation of the phenoxy side chain with respect to the penam unit. The packing motif reveals different pseudosymmetry elements relating certain parts of the unit cell, which may explain the occurrence of this uncommon complex structure. The ^{13}C CP/MAS NMR spectra indicate that the phenyl rings of all the molecules perform apparently uncorrelated 180° flips about their local C_2 axes, at rates on the order of 10^4–10^6 s^{-1} in the temperature range 180–340 K. The anisotropic thermal parameters of the X-ray structural model suggest that these rings also undergo significant librations. Between 352 and 366 K, a phase change to a structure with only two-fold asymmetry is apparent from the ^{13}C CP/MAS NMR spectra. Analysis of the ^{13}C NMR chemical shift anisotropy of the aromatic carbon atoms indicates that pairwise dynamical interchange processes between conformations similar to those present at ambient temperature account for the two-fold asymmetry of the high-temperature crystalline phase. This model enabled the disordered structure of the high-temperature phase to be refined from single-crystal X-ray diffraction data at 373 K. The anisotropic temperature factors of the aromatic rings in the ambient-temperature structure are thought to represent libration of the rings in the direction of the pairwise conformational averaging pathways of the high-temperature structure and therefore indicate restricted pretransitional dynamics. The NMR spectra suggest that the transition proceeds through a homogeneous mechanism. The combination of diffraction and NMR observations has enabled this novel conformational interchange process within a small molecule crystalline solid to be investigated in detail. The results have implications for the understanding of order/disorder transitions in molecular crystals and of conformational interchange dynamics in solids and other close-packed environments.

Introduction

One of the consequences of the widespread application of NMR spectroscopy is that a wide range of molecular dynamic processes has become well-established for molecules in solution. These include stereochemical nonrigidity of small organic and organometallic molecules[1] as well as conformational averaging in macromolecules,[2] including proteins. The utility of NMR to study molecular dynamics arises because the various NMR interactions may be sensitive directly to motions over a wide range of time scales, ca. 10^1–10^{-10} s; NMR is unique in having such an extended range of rates over which it may detect motion explicitly.[3] It is becoming increasingly apparent, especially from solid-state NMR spectroscopy, that molecules can show extensive motional properties, not just in solution but also in the crystalline state. Motions observed to occur in 'ordered' molecular crystals include many of those common in solution, such as fluxionality,[4] pseudorotations,[5] local conformational changes,[6] and overall molecular reorientations.[7] These are revealed in a wide range of effects on NMR spectra, notably through alteration of nuclear relaxation properties[9] and through the effects of motional averaging of NMR parameters.[4-8] Of importance to NMR studies of molecular dynamics in solids has been the increasing use of techniques to characterize the motional behavior not just of molecules as a whole but also of the individual groups within molecules. These techniques include notably CP/MAS NMR methods, to study isotopically or chemically dilute nuclei in a

* To whom correspondence should be addressed.
† Inorganic Chemistry Laboratory.
‡ Present address: Exxon Chemical, Abingdon OX13 6BB, U.K.
§ Chemical Crystallography Laboratory.

(1) Jackman, L. M.; Cotton, F. A. *Dynamic Nuclear Magnetic Resonance Spectroscopy*; Academic Press: New York, 1975. Kowalewski, J. *Annu. Rep. NMR Spectrosc.* **1990**, *22*, 308–414.
(2) Heatley, F. In *Comprehensive Polymer Science*; Allen, G., Bevington, J. C., Eds.; Pergamon Press: Oxford, U.K., 1989; pp 377–396. Wagner, G. *Q. Rev. Biophys.* **1983**, *16*, 1–57. Bovey, F. A.; Jelinski, L. W. *J. Phys. Chem.* **1985**, *89*, 571–583. Dobson, C. M.; Karplus, M. *Methods Enzymol.* **1986**, *131*, 362–389.
(3) Muetterties, E. L. *Inorg. Chem.* **1965**, *4*, 769–771.
(4) Braga, D. *Chem. Rev.* **1992**, *92*, 633–664. Campbell, A. J.; Fyfe, C. A.; Maslowsky, E., Jr. *J. Am. Chem. Soc.* **1972**, *94*, 2690–2692. Lyerla, J. R.; Fyfe, C. A.; Yannoni, C. S. *J. Am. Chem. Soc.* **1979**, *101*, 1351–1353. Meier, B. H.; Earl, W. L. *J. Am. Chem. Soc.* **1985**, *107*, 5553–5555. Benn, R.; Mynott, R.; Topalović, I.; Scott, F. *Organometallics* **1989**, *8*, 2299–2305. Heyes, S. J.; Dobson, C. M. *J. Am. Chem. Soc.* **1991**, *113*, 463–469. Aime, S.; Braga, D.; Gobetto, R.; Grepioni, F.; Orlandi, A. *Inorg. Chem.* **1991**, *30*, 951–956.
(5) Hanson, B. E.; Sullivan, M. J.; Davis, R. J. *J. Am. Chem. Soc.* **1984**, *106*, 251–253. Erker, G.; Nolte, R.; Krüger, C.; Schlund, R.; Benn, R.; Grondey, H.; Mynott, R. *J. Organomet. Chem.* **1989**, *364*, 119–132. Heyes, S. J.; Green, M. L. H.; Dobson, C. M. *Inorg. Chem.* **1991**, *30*, 1930–1937.
(6) Lauprêtre, F.; Virlet, J.; Bayle, J.-P. *Macromolecules* **1985**, *18*, 1846–1850. Meirovitch, E.; Samulski, E. T.; Leed, A.; Scheraga, H. A.; Rananavare, S.; Némethy, G.; Freed, J. H. *J. Phys. Chem.* **1987**, *91*, 4840–4851. Spiess, H. W. *Adv. Polym. Sci.* **1985**, *66*, 23–58.
(7) Fyfe, C. A. *Mol. Cryst. Liq. Cryst.* **1979**, *52*, 1–10. Parsonage, N. G.; Staveley, L. A. K. *Disorder in Crystals*; Clarendon Press: Oxford, U.K., 1978. Ripmeester, J. A.; Ratcliffe, C. I. In *Inclusion Compounds*; Atwood, J. L., Davies, J. E. D., McNicol, D. D., Eds.; Oxford University Press: Oxford, U.K., 1991; Vol. 5, pp 37–89. Johnson, R. D.; Bethune, D. S.; Yannoni, C. S. *Acc. Chem. Res.* **1992**, *25*, 169–175.
(8) Fyfe, C. A. *Solid State NMR for Chemists*; CFC Press: Guelph, Ontario, Canada, 1983, pp 30–71.
(9) Spiess, H. W. In *NMR, Basic Principles and Progress*; Diehl, P., Fluck, E., Kosfeld, R., Eds.; Springer-Verlag: Berlin, 1978; Vol. 15, pp 55–214.

0002-7863/93/1515-5636$04.00/0

solid,[10] and ^2H NMR methods,[11] to study selectively labeled sites in a molecule.

A particular opportunity that arises in the study of crystalline materials is to combine results of NMR experiments with those of diffraction studies. In this regard it is interesting that motional events which do not lead to positional disorder in the crystalline structure may remain undetected by diffraction techniques. This arises because the diffraction process occurs on a time scale on the order of 10^{-18} s, in which period atoms can only move very short distances.[3] Examples of such processes include various fluxional processes of organometallic molecules[6] and the widely studied 180° flip of an aromatic ring about its two-fold axis, which leaves the ring positionally unaltered but permutes atoms at the *ortho* and the *meta* positions. Ring flips have been identified from NMR spectra in a variety of compounds, in both solid and liquid phases, ranging from macromolecular compounds, including polymers[12] and proteins,[13] to small molecular crystals,[14] and need not necessarily be revealed in the diffraction-based structure solutions by enlarged anisotropic thermal parameters.[15] In other cases where dynamic processes lead to disorder in the position of atoms, they will be detected from diffraction techniques by the location of partially occupied atomic positions or in enlarged thermal parameters in the structure solution. Such disorder, however, often leads to a more involved structure solution, even for molecules of a size currently regarded as routine, and may sometimes render a full structure solution impossible. Since the time scales of NMR and diffraction are so disparate, and because NMR interactions are sensitive to local structure whereas diffraction responds to long-range order, the two techniques provide complementary information. In many such cases of disorder, a combination of NMR and diffraction data could perhaps facilitate a full analysis of the structure and of any dynamic events.

The penicillins are a family of antibiotics that have a common structural element of a fused β-lactam/thiazolidine ring system with varying side chains. These molecules provide an excellent opportunity to examine the properties of molecular crystals in a systematic manner. There is a wide range of penicillins,[16] many with well-defined structures because of their relative ease of crystallization. They have elements of common structure, whilst allowing extensive systematic structural variations in a controlled manner. We have shown previously the value of ^{13}C CP/MAS NMR in the study of penicillins, indicating how the methyl region of the spectra predicts reliably the conformation of the thiazolidine ring as C-3 or S-1.[17] The nature of the apparent conformational interconversion between these extremes in aqueous solutions has been confirmed from the ^{13}C CP/MAS NMR spectra of frozen solutions.[18] Also, dynamics of the penicillin side chains, including aromatic ring flips, have been detected and studied in detail[19] by magnetization transfer methods, simulation of exchange-broadened line shapes, and observation of the dipolar broadening mechanism. These studies have yielded kinetic parameters for the ring flip motions in a variety of the penicillins.[19] In the work reported here we discuss a detailed investigation of one member of the penicillin family, potassium penicillin V (KpenV). We have analyzed the ^{13}C CP/MAS spectroscopy of KpenV in the temperature range 180–390 K and have determined its structure, at both 293 and 373 K, from single-crystal X-ray diffraction data. KpenV shows not only the localized dynamic properties increasingly familiar for such molecules but also a remarkable dynamic phase transition at 356 K. The combined approach of solid-state NMR spectroscopy and X-ray diffraction for this molecule allows an unusually informative investigation of structural and dynamical aspects of a molecular crystal and provides substantial insight into properties of molecular crystals that are of general interest and applicability, as well as illustrating how NMR and diffraction techniques combine in a synergic manner.

Experimental Section

(i) **Preparation and Characterization of KpenV.** Microcrystalline samples of KpenV ($C_{16}H_{17}N_2O_5SK$, M_r 388.5) were purchased from the Sigma Chemical Co. and were also kindly donated by Dr. J. Everett and Mr. A. E. Bird of SmithKline Beecham Pharmaceuticals, Brockham Park, Surrey, U.K. Samples of material from both sources gave X-ray powder diffractograms (A Phillips PW1710 diffractometer, using Cu Kα radiation, was employed, and reflections were internally referenced and checked against a silicon standard) which were consistent with the unit cell parameters determined from preliminary unpublished single-crystal X-ray diffraction work.[20] Samples were used for NMR, DSC, and variable-temperature X-ray powder diffraction experiments without further purification.

(ii) **Solid-State NMR Spectroscopy.** ^{13}C CP/MAS NMR spectra were acquired on a Bruker MSL 200 spectrometer equipped with an Oxford Instruments 4.7-T wide-bore (98 mm) superconducting solenoid magnet operating at frequencies of 50.32 and 200.13 MHz for ^{13}C and ^1H, respectively. Acquisition and processing of data were controlled by an Aspect 3000 computer. CP/MAS spectra were recorded using a multinuclear, proton-enhanced, double-bearing magic angle sample spinning probe (Bruker Z32-DR-MAS-7DB), utilizing dry nitrogen for all gas requirements. Approximately 250 mg of sample was packed into 7-mm zirconia rotors with Kel-F caps for MAS at typical rates of 1–4 kHz. A single-contact spin-lock cross polarization (CP) sequence[21] with alternate cycle spin-temperature inversion,[22] with flip-back of ^1H magnetization,[23] and with a proton radiofrequency field of 1.7 mT ($\omega_1 \approx 75$ kHz), resulting in a 90° pulse length of 3.5 μs, was used. Temperature measurement and regulation, utilizing a Bruker B-VT1000 unit equipped with a copper-constantan thermocouple and digital reference, was of the bearing gas. Temperature calibration was achieved both with the samarium ethanoate tetrahydrate Curie Law ^{13}C NMR chemical shift thermometer,[24] previously set against the phase transitions of *d*-camphor,[24] cobaltocenium hexafluorophosphate,[25] and 1,4-diazabicyclo[2.2.2]-octane,[24] and with the samarium stannate, $Sm_2Sn_2O_7$, Curie Law ^{119}Sn

(10) Schaefer, J.; Stejskal, E. O. In *Topics in Carbon-13 NMR Spectroscopy*; Levy, G. C., Ed.; Wiley: New York, 1979; Vol. 3, pp 283–324. Wind, R. A. In *Modern NMR Techniques and their Application to Chemistry*; Popov, A. I., Hallenga, K., Eds.; Marcel·Dekker: New York, 1991; pp 125–215.

(11) Spiess, H. W. *Adv. Polym. Sci.* **1985**, *66*, 23–58. Spiess, H. W. *Chem. Rev.* **1991**, *91*, 1321–1338. Wittebort, R. J.; Olejniczak, E. T.; Griffin, R. G. *J. Chem. Phys.* **1987**, *86*, 5411–5420. Clayden, N. J.; Dobson, C. M.; Heyes, S. J.; Wiseman, P. J. *J. Inclusion Phenom.* **1987**, *5*, 65–68. Sarkar, S. K.; Young, P. E.; Torchia, D. A. *J. Am. Chem. Soc.* **1986**, *108*, 6459–6464.

(12) Garroway, A. N.; Ritchey, W. M.; Moniz, W. B. *Macromolecules* **1982**, *15*, 1051–1063. Schaefer, J.; Sefcik, M. D.; Stejskal, E. O.; McKay, R. A.; Dixon, W. T.; Cais, R. E. *Macromolecules* **1984**, *17*, 1107–1118. Schaefer, J.; Stejskal, E. O.; McKay, R. A.; Dixon, W. T. *Macromolecules* **1984**, *17*, 1479–1489. Schaefer, J.; Stejskal, E. O.; Perchak, D.; Skolnick, J.; Yaris, R. *Macromolecules* **1985**, *18*, 368–373. Speiss, H. W. *Colloid Polym. Sci.* **1983**, *261*, 193–209.

(13) Campbell, I. D.; Dobson, C. M.; Moore, G. R.; Perkins, S. J.; Williams, R. J. P. *FEBS Lett.* **1976**, *70*, 96–100. Wagner, G. *FEBS Lett.* **1980**, *112*, 280–284. Wüthrich, K. *NMR in Biological Research: Peptides and Proteins*; Elsevier: Amsterdam, The Netherlands, 1976. Rice, D. M.; Wittebort, R. J.; Griffin, R. G.; Meirovitch, E.; Stimson, E. R.; Meinwald, Y. C.; Freed, J. H.; Scheraga, H. A. *J. Am. Chem. Soc.* **1981**, *103*, 7707–7710.

(14) Clayden, N. J. *J. Chem. Soc., Perkin Trans. II* **1990**, 729–733. Frey, M. H.; DiVerdi, J. A.; Opella, S. J. *J. Am. Chem. Soc.* **1985**, *107*, 7311–7315. Schaefer, J.; Stejskal, E. O.; McKay, R. A.; Dixon, W. T. *J. Magn. Reson.* **1984**, *57*, 85–92. Harbison, G. S.; Raleigh, D. P.; Herzfeld, J.; Griffin, R. G. *J. Magn. Reson.* **1985**, *64*, 284–295. Hiyama, Y.; Silverton, J. V.; Torchia, D. A.; Gerig, J. T.; Hammond, S. J. *J. Am. Chem. Soc.* **1986**, *108*, 2715–2723.

(15) Twyman, J. M.; Baird, P. D.; Prout, C. K.; Dobson, C. M. Unpublished observations.

(16) Morin, R. B.; Gorman, M. *β-Lactam Antibiotics, Chemistry and Biology*; Academic Press: New York, 1981.

(17) Clayden, N. J.; Dobson, C. M.; Lian, L.-Y.; Twyman, J. M. *J. Chem. Soc., Perkin Trans. II* **1986**, 1933–1940.

(18) Twyman, J. M.; Fattah, J.; Dobson, C. M. *J. Chem. Soc., Chem. Commun.* **1991**, 647–649.

(19) Twyman, J. M.; Dobson, C. M. *J. Chem. Soc., Chem. Commun.* **1988**, 786–788. Twyman, J. M. D.Phil Thesis, University of Oxford, U.K., 1989. Twyman, J. M.; Dobson, C. M. *Magn. Reson. Chem.* **1990**, *28*, 163–170.

(20) Hodgkin, D. C. Personal communication.

(21) Pines, A.; Gibby, M. G.; Waugh, J. S. *J. Chem. Phys.* **1973**, *59*, 569–590. Yannoni, C. S. *Acc. Chem. Res.* **1982**, *15*, 201–208.

(22) Stejskal, E. O.; Schaefer, J. *J. Magn. Reson.* **1975**, *18*, 560–563.

(23) Tegenfeldt, J.; Haeberlen, U. *J. Magn. Reson.* **1979**, *36*, 453–457.

(24) Haw, J. F.; Campbell, G. C.; Crosby, R. C. *Anal. Chem.* **1986**, *58*, 3172–3177.

(25) Heyes, S. J. D.Phil Thesis, University of Oxford, U.K., 1989.

NMR chemical shift thermometer.[26] Spectra were generally recorded with 3–5 K temperature increments, and ca. 20 min was allowed for equilibration at each new temperature before commencement of spectral acquisition. Free induction decays were defined by ca. 2K data points over a spectral width of 20 kHz and were zero-filled to 8K data points prior to Fourier transformation. Typically 100–1000 transients, with a contact time of 0.75 ms and a relaxation delay of 5–8 s, were accumulated for each spectrum. Chemical shifts are reported on the δ scale with respect to δ(TMS) = 0 ppm and were referenced externally to the upfield resonance of solid adamantane at 29.5 ppm.[27] The ^{79}Br NMR spectrum of a small quantity of KBr included with the adamantane sample was used to calibrate accurately the magic angle.[28] Dipolar dephasing experiments,[29] using delays of 20–200 μs, were carried out using the pulse sequence of Alemany et al.[30] in which 180° pulses are simultaneously applied to the proton and carbon spins half way through the delay time in order to refocus the effects of chemical shifts and other static field inhomogeneities.

The principal components of the chemical shift tensors were recovered from the spinning sideband manifold, measured in at least two slow spinning speed MAS NMR spectra, by using the Maricq and Waugh moment analysis.[31] Iterative comparison of the experimental and simulated MAS NMR spectra, using a downhill *SIMPLEX* algorithm,[32] was then used for refinement of the tensor components,[33] and such refined values are quoted with error limits derived from the fitting process. The Herzfeld-Berger[35] convention for the labeling of sidebands is employed here. The conventional assignment for labeling of the principal components of the CSA tensor is used, employing $\delta_{11} \geq \delta_{22} \geq \delta_{33}$ to denote use of the δ chemical shift scale. The parameter $\Delta\delta = (\delta_{11} - \delta_{33})$ is used[36] as a measure of the spread of the CSA, and together with the asymmetry parameter, $\eta = (\delta_{11} - \delta_{22})/(\delta_i - \delta_{33})$ if $(\delta_i - \delta_{33}) > (\delta_{11} - \delta_i)$ or $\eta = (\delta_{22} - \delta_{33})/(\delta_{11} - \delta_i)$ if $(\delta_i - \delta_{33}) < (\delta_{11} - \delta_i)$ (where $0 \leq \eta \leq 1$), characterizes any changes to the CSA caused by motional averaging.

(iii) **Single-Crystal X-ray Diffraction.** Single-crystals of KpenV were grown by vapor diffusion of acetone into aqueous alcohol solutions. Preliminary X-ray photography of most of these crystals showed the presence of twinning, though fortunately a suitable untwinned single crystal was eventually identified. The crystallization procedure by which this was achieved differed only slightly from those procedures which consistently yielded twinned crystals. KpenV (99.0 mg) was dissolved in distilled water (0.18 cm^3). Isopropyl alcohol (100 μL) was added, and the clear solution was left to stand in an acetone bath in a closed container at 296 K. Crystal growth was observed after 3 to 4 h. After 24 h a number of crystals were removed from the mother liquor and mounted on fine glass fibers. Following preliminary X-ray photographic diffraction analysis, one of these crystals was examined on an Enraf-Nonius CAD4 diffractometer using graphite monochromated Cu Kα radiation. Analysis prior to collection of a full data set gave satisfactory unit cell dimensions based on 25 strong reflections. The observed intensity data were corrected for Lorentz and polarization factors and for absorption. Diffraction data were collected at two temperatures, 293 and 373 K. Details of the data collection are given in Table I.

The structures were solved by direct methods. The resolution of the structure from the room-temperature data proved problematical. The "E-maps" produced by both SIR88[37] and SHELXS86[38] did not allow solution of the structure (see Figure 1). This problem was eventually resolved using the CRYSTALS[39] program driven by a novel protocol. From the solid-state NMR spectroscopic studies and the crystallographically calculated density, the asymmetric unit of the structure was known to contain four independent molecules and therefore 100 non-hydrogen atoms. Therefore the 100 highest peaks from the E-map computed with the phases of the highest overall figure of merit solution from SIR88 were used as a starting point.

Table I. Crystal Data for Potassium Penicillin V in Ambient- and High-Temperature Phases

	KPenV	
crystal and experimental data	293 K	373 K
crystal system	triclinic	triclinic
space group	*P*1 (No. 1)	*P*1 (No. 1)
a/Å	9.377(2)	9.387(2)
b/Å	12.517(5)	6.289(1)
c/Å	15.384(2)	15.518(4)
α/deg	93.73(2)	94.36(2)
β/deg	99.30(1)	99.07(2)
γ/deg	89.71(2)	90.09(2)
cell vol/Å^3	1778	902
Z	4	2
ρ/g cm^{-3}	1.45	1.43
no. of reflns used for cell refinement	24	25
θ limits for cell/deg	$8.77 \leq \theta \leq 56.33$	$25.4 \leq \theta \leq 43.3$
instrument	Enraf-Nonius CAD4	Enraf-Nonius CAD4
radiation	Cu Kα	Cu Kα
scan mode	ω:2θ	ω:2θ
θ range for data collection	$0 < 2\theta \leq 150°$	$0 < 2\theta \leq 150°$
no. of reflns collected	8639	5927[a]
no. of unique reflns	7166	5039
R-merg	0.039	0.052
no. of parameters refined	901	399
no. of observed $I \geq 3\sigma I$	5580	2687
temperature/K	293 ± 2	373 ± 5
crystal dimensions/mm	0.2 × 0.4 × 0.8	0.2 × 0.4 × 0.8
reflns measured	$-11 \leq h \leq 11$	$-11 \leq h \leq 11$
	$-15 \leq k \leq 15$	$-15 \leq k^a \leq 15$
	$-1 \leq l \leq 19$	$-1 \leq l \leq 19$
min, max absorption corrections	1.70, 1.80	1.70, 1.80
μ/cm^{-1}	39.90	39.30
residual electron density/eÅ^{-3}	min –0.84	min –0.79
	max 0.83	max 0.55
final *R*, R_w	0.061, 0.075	0.114, 0.128

[a] *k* odd was measured for the doubled *b*-axis for the first 55° shell, but not in the 55–75° shell.

The initial positions were subjected to a Fourier synthesis, computed using $2F_o - F_c$[40] as the coefficients and with Sim weighting,[41] using all reflections. The resulting map was searched for peaks, which were ranked in order of electron density. The 100 highest peaks were retained, with the four densest being assigned as potassium atoms, the next four as sulfur atoms, and the remainder as carbon. This protocol acts as a means of finding new atomic positions and retaining or rejecting old ones and, in particular, acts as a means of creating new positions, since it stresses those areas of electron density unaccounted for by the initial trial solution. After three iterations of this procedure a full matrix least squares refinement of positional and isotropic thermal parameters was performed, using only reflections for which $I > 10\sigma(I)$. During refinement U_{iso} was prevented from becoming negative, and the maximum shift on any cycle was restrained to be 0.05 Å^2. The number of cycles of refinement permitted was between 4 and 8, selected automatically as a function of the success of the refinement. At the end of the refinement stage, those atoms with U_{iso} greater than 0.1 Å^2 were rejected as spurious. This overall procedure was then repeated twice. On completion of this computation[42] all the non-hydrogen atoms had been located, and the *R*-factor stood at 0.15. E-maps before and after this process are shown in Figure 1.

For the least squares refinement of positional and anisotropic thermal parameters for all non-hydrogen atoms of the model at $R = 0.15$, due

(26) Grey, C. P.; Cheetham, A. K.; Dobson, C. M. *J. Magn. Reson.* **1993**, *101*, 299–306.
(27) Earl, W. L.; VanderHart, D. L. *J. Magn. Reson.* **1982**, *48*, 35–54.
(28) Frye, J. S.; Maciel, G. E. *J. Magn. Reson.* **1982**, *48*, 125–131.
(29) Opella, S. J.; Frey, M. H. *J. Am. Chem. Soc.* **1979**, *101*, 5854–5856.
(30) Alemany, L. B.; Grant, D. M.; Alger, T. D.; Pugmire, R. J. *J. Am. Chem. Soc.* **1983**, *105*, 6697–6704.
(31) Maricq, M. M.; Waugh, J. S. *J. Chem. Phys.* **1979**, *70*, 3300–3316.
(32) Nedler, J. A.; Mead, R. *Comput. J.* **1965**, *7*, 308–313.
(33) The MAS NMR spectrum at each MAS rate was simulated by using eq 30 of Maricq and Waugh[31,34] to evaluate the MAS FID from the tensor information. Powder averaging was performed in 2° steps, and the rotational echo was replicated to give 1024 points; the FID was convoluted with Gaussian and Lorentzian functions of choice and zero-filled to 8K points.
(34) Clayden, N. J.; Dobson, C. M.; Lian, L.-Y.; Smith, D. J. *J. Magn. Reson.* **1986**, *69*, 476–487.
(35) Herzfeld, J.; Berger, A. E. *J. Chem. Phys.* **1980**, *73*, 6021–6030.
(36) Mehring, M. *Principles of High Resolution NMR in Solids*, 2nd ed.; Springer-Verlag: Berlin, 1983; pp 25–30.
(37) Burla, M. C.; Camalli, M.; Cascarano, G.; Giacovazzo, C.; Polidori, G.; Spagna, R.; Viterbo, D. *J. Appl. Crystallogr.* **1989**, *22*, 389–393.
(38) Sheldrick, G. M. In *Crystallographic Computing 3*; Sheldrick, G. M., Kruger, C., Goddard, R., Eds.; Oxford University Press: Oxford, U.K., 1985; pp 175–189.
(39) Watkin, D. J.; Carruthers, J. R.; Betteridge, P. W. CRYSTALS User Guide, Chemical Crystallography Laboratory: Oxford, U.K., 1985.
(40) Ramachandron, G. N.; Raman, S. *Acta Crystallogr.* **1959**, *12*, 957–964.
(41) Sim, G. A. *Computing Methods and the Phase Problem in X-Ray Crystal Analysis*; Pergamon Press: Oxford, U.K., 1961.
(42) This process took 10 h of CPU time on a Microvax 3800. Recently, reprocessing of the data using 'active' data files, which permit logical control of the process, subject to making numerical decisions has resolved the structure in 5 h on the same computer.

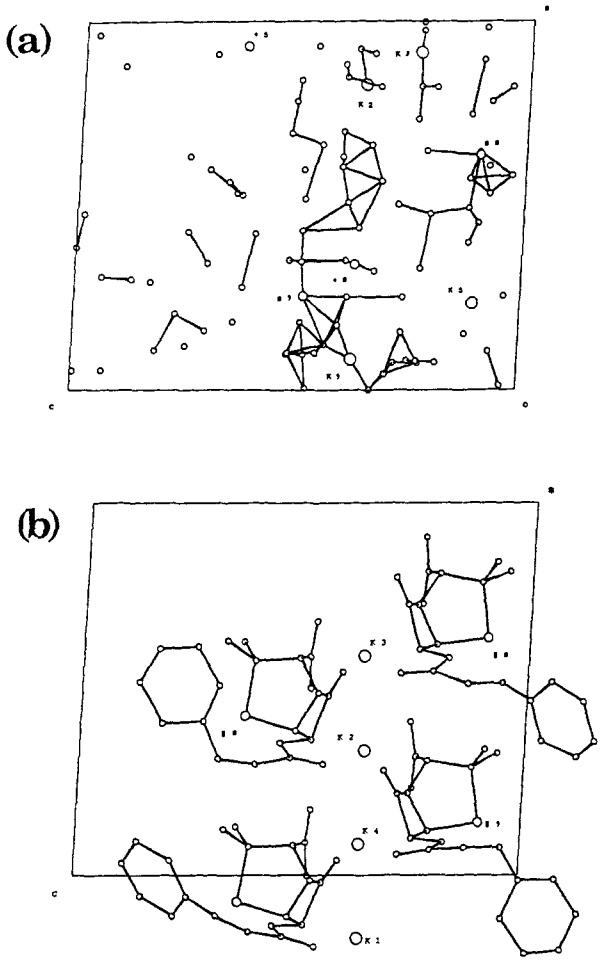

Figure 1. E-Maps for the single-crystal X-ray diffraction study of potassium penicillin V at 293 K: (a) E-map generated by *SIR*; (b) E-map after application of the new *CRYSTALS* protocol described in the Experimental Section, showing the structure solution.

to the size of the structure, a block approximation to the full matrix was employed. In the initial stages of this refinement, distance, angle, and thermal motion restraints were applied to the side chains of each of the four molecules of the asymmetric unit, but only restraints on thermal motion in the side chains and shift-limiting restraints were applied in the final stages. Hydrogen atoms were included in the model at calculated positions and were assigned thermal parameters equal to the U_{eq} of the atom to which they were attached. Refinement of the 901 parameters coverged to $R = 0.061$, $R_w = 0.075$.

For the high-temperature structure at 373 ± 5 K, the crystal used for the room-temperature data collection was transferred to a Lindemann glass capillary which was mounted in 'CETAC' dental cement. The temperature was raised by means of a small thermostatically controlled hot nitrogen gun and was monitored with a thermocouple placed in the exit stream. The diffraction pattern was monitored photographically as the temperature was slowly raised and no deterioration was observed. Initial indexing of 25 strong reflections indicated a unit cell with a, c, α, β, and γ dimensions similar to those of the ambient-temperature structure, but the length of the unit cell b-axis was approximately halved. It was considered necessary to transform the cell to that with a doubled b-axis for the first shell ($0 < 2\theta < 55°$) of data collection in order to confirm the absence of all reflections hkl with k odd. This both verified the halving of the b-axis relative to ambient temperature and monitored the maintenance of the crystal in the high-temperature phase. At no time was any reflection with k odd observed, and the remainder of the data set was collected only for k even. Some reflections, intense at ambient temperature and with $k = 2n + 1$, were measured on repeated thermal cycling to demonstrate conclusively the rapid and reversible halving of the b-axis at the phase change. Details of the data collection are collected in Table I. Direct methods computations using *SHELXS*[38] readily yielded a structure solution for all but the $CH_2OC_6H_5$ groups of the two molecules in the asymmetric unit. This model was refined, and examination of

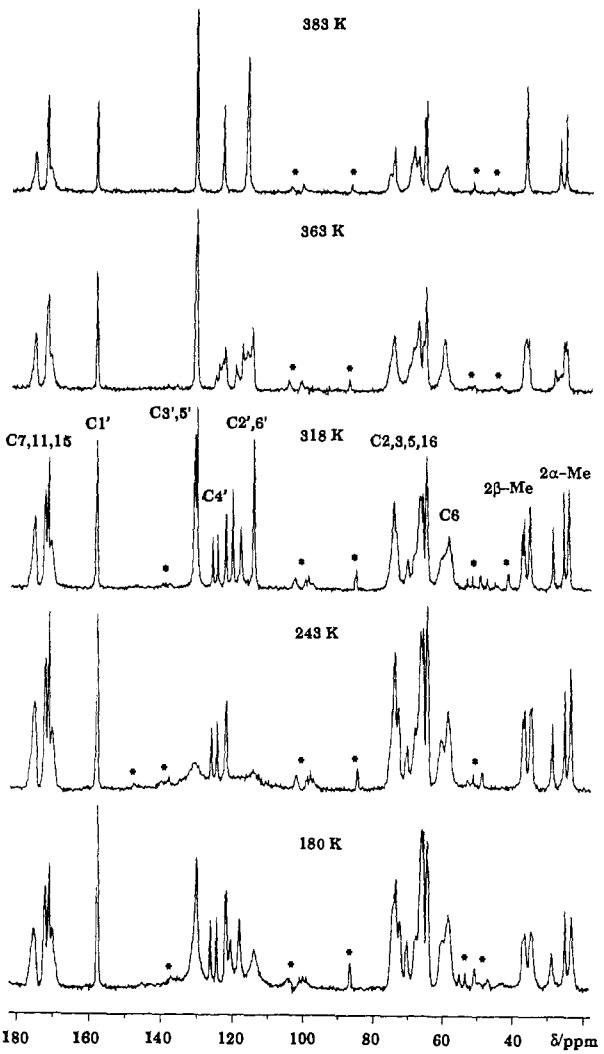

Figure 2. ^{13}C CP/MAS NMR spectra of potassium penicillin V in the temperature range 181–383 K. * denotes spinning sideband.

Fourier electron density maps showed regions of significant but diffuse electron density in sites where the phenyl rings were assumed to be located. The structure solution was completed using methods described in the Results and Discussion section.

(iv) **Differential Scanning Calorimetry.** DSC was performed on ca. 20 mg of KpenV using a Perkin-Elmer 7 Series Thermal Analysis System. Results were obtained from heating and cooling cycles between 296 and 400 K, typically at rates of 5 K/min and in the presence of a nitrogen gas purge.

(v) **Variable-Temperature X-ray Powder Diffraction.** X-ray powder patterns were obtained in the temperature range 297–400 K on a STOE 7 powder diffractometer using monochromated Cu $K\alpha_1$ radiation. High-temperature data were obtained using a home-built heating device, designed specifically for these experiments and positioned with the heat source directly below the sample. The temperature was calibrated to an accuracy of ≈±5 K.

Results and Discussion

(i) ^{13}C CP/MAS NMR Spectroscopy. ^{13}C CP/MAS NMR spectra of KpenV in the temperature range 180–390 K are shown in Figure 2. Identical spectra were obtained for all samples. Above ambient temperature they show well-resolved ($\Delta\nu_{1/2} < 20$ Hz), widely dispersed resonances of good signal-to-noise ratio; bands of resonances from carbons of distinct functional groups are immediately identified. Detailed assignments were made from dipolar-dephased spectra, which reveal resonances from quaternary and methyl carbon atoms, and by comparison with spectra of structurally related compounds.[17-19] The notation used in the discussion of the NMR results is illustrated in Table 4.

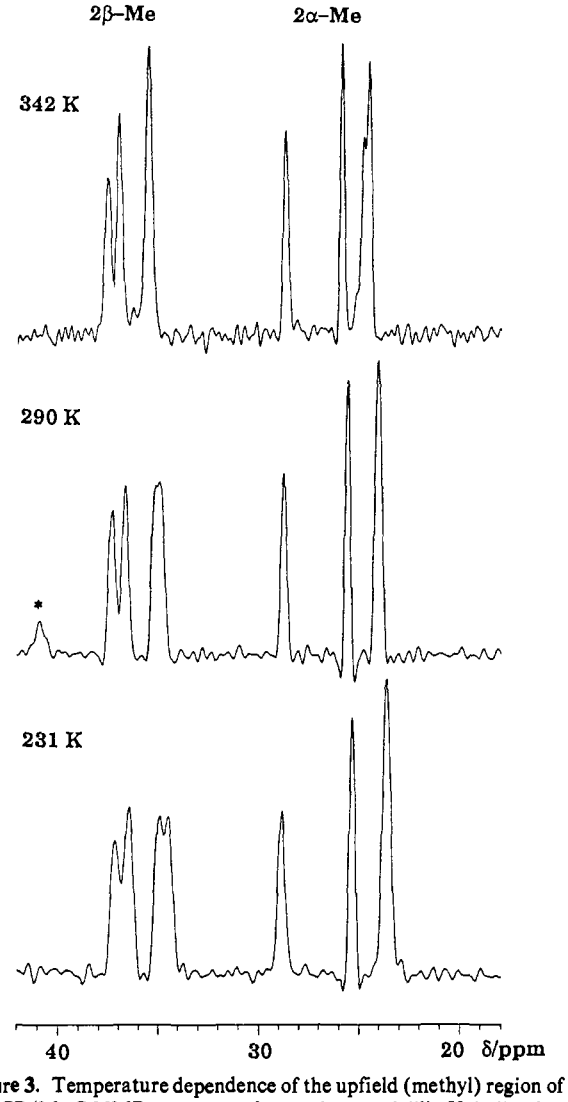

Figure 3. Temperature dependence of the upfield (methyl) region of the ^{13}C CP/MAS NMR spectrum of potassium penicillin V, indicating the presence of at least four molecules in the asymmetric unit of the crystalline structure. * denotes spinning sideband.

(a) Ambient-Temperature Form ($T \leq 350$ K). Examination of the spectra reveals immediately a significantly greater number of peaks than the number of chemically distinct carbon sites in the molecule. The peak multiplicities and intensities of the resonances are most consistent with an interpretation demanding the presence of at least four distinct molecules in the crystallographic asymmetric unit, as suggested originally by Hodgkin.[20] This is a significant observation, since ^{13}C CP/MAS NMR spectra of a wide range of penicillins[17,19] have indicated structures with a single molecule in the asymmetric unit.

The four-fold multiplicity of resonances is apparent particularly in the upfield region of the spectrum (Figure 3), which at ambient temperature consists of six peaks due to the two chemically distinct methyl carbons of the molecule; the resonances at 24.1 and 34.9 ppm are of twice the intensity of the others. In a combination of spectra at higher and lower temperatures, the accidental degeneracies leading to the peaks of double intensity are lifted and the full four-fold nature of each methyl resonance is revealed. The four most upfield peaks are assigned to the 2α-methyl carbon atoms, and the four downfield peaks are in the chemical shift range associated previously with the 2β-methyl carbons of a thiazolidine ring in a C-3 conformation.[17]

The aromatic region of the spectrum shows a number of resonances of significantly varying intensity and line width, which indicates the presence of significant molecular dynamic events. Full information may only be extracted from this region of the spectrum on an extensive variable-temperature study of the resonance profile, as shown in Figure 4.

On increasing temperature from 180 to ca. 240 K, the majority of aromatic carbon peaks broaden, becoming virtually indistinct from the baseline around 240 K. Above this temperature the broadened resonances narrow progressively until by ≈310 K they are as sharp as the others. Similar spectral behavior has been observed before in penicillin V (free acid, benzyl ester, benzyl ester β-sulfoxide), sodium carfecillin, and potassium penicillin G.[19] It has been interpreted as indicative of a 180° aromatic ring reorientation or 'flip' motion. Such a ring flip motion gives rise in the ^{13}C CP/MAS spectrum to the equivalence in the *ortho* (C2′,C6′) pair and *meta* (C3′,C5′) pair of resonances in the fast limit on the exchange-broadening time scale. The *ipso* (C1′) and *para* (C4′) resonances are unaffected by this event. The spectra of KpenV at all temperatures above 180 K are consistent with ring flip motion in the fast limit, such that only averaged C2′,6′ and C3′,5′ resonances are observed. In CP/MAS NMR, motions on the time scale of the magic angle sample spinning may interfere with the averaging by MAS of the chemical shift anisotropy (CSA)[43] and motion on the order of the ^{1}H high-power radiofrequency decoupling field strength (ω_1) may interfere with the dipolar decoupling.[44] In both cases a region of broadening is expected due to reintroduction of the ^{13}C CSA and dipolar coupling to protons, respectively. The substantial broadening of the aromatic resonances in KpenV around ca. 240 K is identified with the reintroduction of dipolar broadening due to destructive interference between the decoupling actions of the coherent resonant ^{1}H radiofrequency field ($\omega_1 \approx 75$ kHz) and the incoherent averaging due to the ring flip dynamics. The maximum broadening effect from this mechanism is expected to occur when the motional and radiofrequency field frequencies are identical (i.e. $\omega_1 \tau_c = 1$).[44] Inspection of the spectra in this regime allows assignment of the resonances in the region 122–127 ppm, which remain unbroadened, to C4′ carbons. From comparison with ^{13}C NMR spectra in solution, the resonances in the area 113–121 ppm are assigned to the averaged (C2′,C6′) pairs, and those between 128 and 135 ppm to the (C3′,C5′) pairs. In the spectrum at 296 K the resonances at 120.3, 117.9, and 114.2 ppm are therefore assigned to the C2′,6′ carbons; the peak at 114.2 ppm is of double intensity (only at 340 K is this accidental degeneracy lifted such that four distinct peaks from the C2′,6′ pairs are identified). The chemical shift spread of the peaks due to the C3′,5′ carbon atoms is considerably smaller, and the crystallographic inequivalences are not resolved. That line broadening of the C1′ and C4′ phenoxy carbon resonances is not observed is clearly consistent with the model of 180° phenoxy ring flips about the local C_2 symmetry axes of the rings.

Even at temperatures as low as 180 K, the aromatic ring flip is at a rate in the fast limit on the exchange-broadening time scale, and importantly, above ca. 310 K it is fast on all the pertinent NMR time scales (exchange-broadening, MAS, and dipolar-decoupling regimes). Analyses based on magnetization transfer experiments, simulation of exchange-broadened line shapes, and determination of the extent of dipolar-induced broadening have enabled the activation parameters for the aromatic ring flips to be determined for a number of other crystalline penicillins.[19] A full kinetic analysis of the ring flip rates proves not to be feasible in this case, due to the complexity introduced by the four-fold asymmetry. The lack of spectral resolution in the region of dipolar broadening precludes a precise determination of individual ring flip rates and makes an estimate of the precise temperature of maximum line broadening for each individual peak impossible. In the case of the benzyl ester β-sulfoxide of penicillin V, the two chemically distinct aromatic rings in the structure are shown to

(43) Suwelack, D.; Rothwell, W. P.; Waugh, J. S. *J. Chem. Phys.* **1980**, *73*, 2559–2569.
(44) Rothwell, W. P.; Waugh, J. S. *J. Chem. Phys.* **1981**, *74*, 2721–2732.

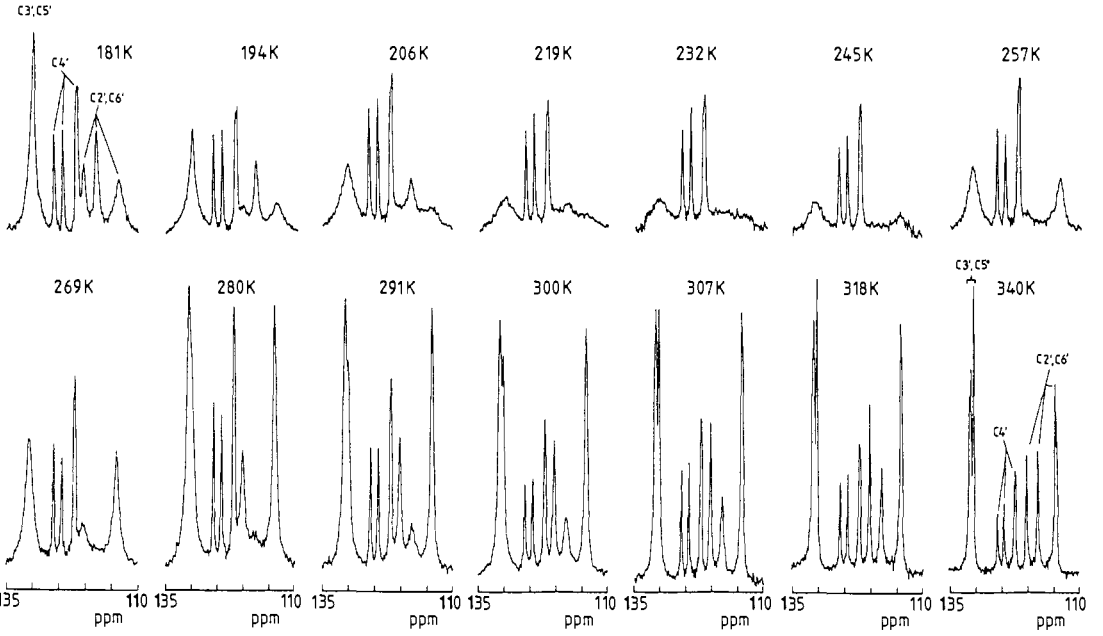

Figure 4. Temperature dependence of the aromatic region of the ^{13}C CP/MAS NMR spectrum of potassium penicillin V. The region of dipolar line broadening of the C2′,6′ and C3′,5′ resonances is clearly evident.

have widely different activation parameters for ring flips.[19] By comparison the ring flip processes for the four independent molecules of potassium penicillin V may be regarded as very similar. However, the temperature dependences of the line-shape profiles of each of the resolved C2′,6′ peaks are clearly different. The rings represented by the resonance at 117.9 ppm reorient at a slower rate, and the ring represented by the resonance at 114.2 ppm flips faster than the others at any given temperature. This implies that the ring flip rates for the different molecules in the structure are not correlated and therefore not linked by a concerted process.

In summary, these spectra indicate the presence of four distinct penicillin V molecules in the structure of KpenV. In each case the phenoxy rings of the molecules are executing 180° flips of gradually increasing rate with rise in temperature. The ring flips of the different molecules in the structure are apparently not correlated, but all have rates on the order of 10^4–10^6 s^{-1} in the temperature range 180–350 K.

(b) Phase Transition and High-Temperature Form ($T \geq 366$ K). Figure 5 details the spectra of KpenV in the range 342–383 K; these spectra show changes consistent with a solid-state transition between crystalline phases. As the temperature is increased, at 356 K new low-intensity peaks, which are particularly apparent in the methyl and aromatic spectral regions, can be seen in the spectrum. As the temperature is raised further, the intensities of these additional peaks increase relative to those of the original peaks, until at 370 K the new peaks have completely replaced the originals. The spectra at ≥370 K reveal a two-fold multiplicity of resonances associated with each chemically distinct intramolecular carbon site (e.g. the resonances of C1′, C3′,5′, C2′,6′, 2α-Me), suggesting an underlying two-fold crystallographic asymmetry and contrasting with the spectra recorded below 350 K, where a four-fold multiplicity of resonances was observed. Cooling the sample from 383 K to below 356 K yields at each temperature spectra similar to those obtained on heating. No temperature hysteresis is observed, and the phase transition appears to be fully reversible. An interesting observation is that the spectra in the regime of the phase transition appear not to be just a simple superposition of the resonances of low- and high-temperature forms. The resonances of the high-temperature form are proportionately broader at lower temperatures, and the resonances of the low-temperature form show fine structure and increased dispersion, in the presence of the high-temperature phase. These observations are of importance regarding the intimate nature of the phase transition, and this is discussed at greater length below.

The occurrence of the phase transition in this bulk material is confirmed by other measurements. DSC detects a thermal event with an onset temperature on heating of 353 K, which is fully reversible on cooling. Powder X-ray diffraction patterns at 296 and 396 K are very different, suggesting distinctly different crystalline structures at the two temperatures and a considerably smaller unit cell in the high-temperature form. The diffraction patterns confirm that, as was apparent from the narrow line widths of the NMR spectra in low- and high-temperature forms, crystallinity of the phases is retained during thermal cycling through the transition, as was also found for a single crystal.

For the aromatic carbon resonances of the ^{13}C CP/MAS NMR spectra at all temperatures, residual CSA is evident in the form of significant spinning sidebands. Comparison of the spinning sideband manifolds of the C2′,6′, C3′,5′, and C4′ resonances provides an indication of the relative magnitudes of the ^{13}C NMR CSAs at the different sites. From inspection alone it appears that the relative sideband intensities are greater for the C4′ sites than for either the C2′,6′ or the C3′,5′ aromatic sites. In the high-temperature form the sideband intensities of the resonances of all of these sites are reduced substantially in comparison with those of the low-temperature phase.

The principal values of the CSA tensor for C2′,6′ and for C4′ aromatic sites were determined from analysis of the sideband spectra at low MAS rates[31,35] in both low- and high-temperature phases. Due to extensive spectral overlap, the range of MAS rates appropriate for such a procedure is limited, and the maximum number of sidebands observable in each instance was consequently restricted. The high resolution and good signal-to-noise ratio of the spectra obtained do, however, lead to data suitable for a reliable analysis. Figure 6 shows experimental spectra at 304 and 380 K together with sideband simulations for selected C2′,6′ and C4′ peaks. The anisotropic chemical shift parameters are summarized in Table II.

At 304 K the anisotropy is indeed much smaller for the *ortho*, C2′,6′, carbons ($\Delta\delta \approx 152$ ppm) than for the *para*, C4′, carbons ($\Delta\delta \approx 205$ ppm). The CSAs of the C4′ resonances are typical of those of static aromatic carbon atoms.[45,46] From single-crystal studies of a range of aromatic compounds, Veeman[45] has proposed that the CSA tensors of aromatic carbon atoms are oriented in

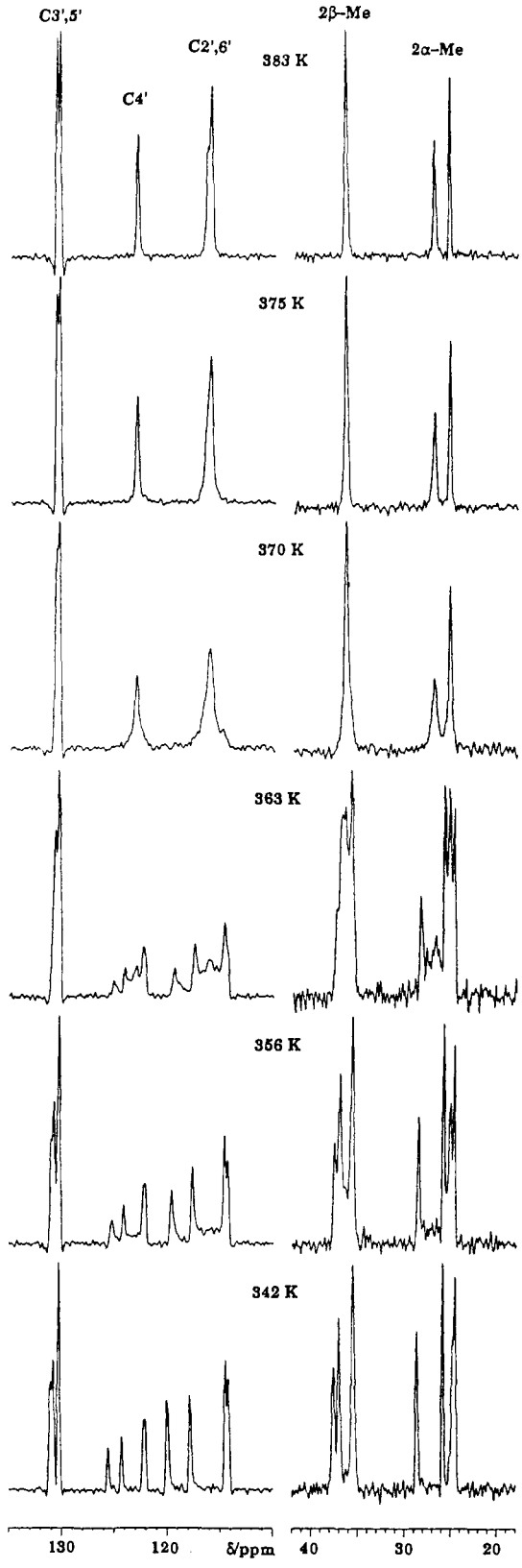

Figure 5. ^{13}C CP/MAS NMR spectra of potassium penicillin V in the temperature range 342–383 K, focusing on the methyl and aromatic regions of the spectrum and illustrating the occurrence of the phase change.

the molecular frame such that the most shielded component, δ_{33}, is perpendicular to the plane of the ring, the least shielded orientation, δ_{11}, is along the bond to the substituent group, and δ_{22} is in the plane of the ring. In this case the orientations of the static CSA tensors of the C4′ carbons of KpenV will not be altered by the 180° ring flip process. The CSAs at the C2′,6′ sites, however, are expected to be reduced substantially from their rigid lattice values, as a result of the change in orientation with respect to the static magnetic field.[47] Assuming the standard tensor orientation and also that the anisotropy and asymmetry parameter as measured for C4′ are similar to the effectively 'static' values pertaining to the C2′,6′ resonance, the effect of a ring flip on the CSA of the latter may be computed by using order parameter theory.[48] The calculated values of δ_{11} = 196, δ_{22} = 157, and δ_{33} = 9 ppm suggest that this view is essentially correct (the reduction in δ_{11} and the increase in δ_{33}, each by 20 ppm, in the observed tensor could be explained if the static tensor were tilted slightly away from the model orientation), and the ambient-temperature tensor values are therefore consistent with 180° ring flips. For all the aromatic carbon atoms, the CSAs are significantly reduced in the higher temperature phase. These reductions require the presence of further dynamic averaging in addition to the ring flip motions. The extent of the reduction of the anisotropy of the C4′ carbon atoms from $\Delta\delta \approx 205$ ppm at 304 K to ≈140 ppm at 370 K implies a significant conformational averaging involving the phenoxy rings. The reduction in the asymmetry of the structure from four-fold to two-fold that accompanies this increased motional freedom suggests in the high-temperature form a possible pairwise interconversion of the molecular forms present in the low-temperature structure, such that interchange occurs between conformations within a pair but not between conformations of the different pairs. The nature of these changes is probed further by single-crystal X-ray diffraction experiments, and an interpretation based upon the combination of the complementary techniques of NMR spectroscopy and diffraction is presented.

(ii) Single-Crystal X-ray Diffraction. (a) Ambient-Temperature Structure. The structure of potassium penicillin V was solved and subsequently refined from the X-ray diffraction data of an untwinned crystal using the novel protocol described in the Experimental Section. KpenV crystallizes in the space group *P*1 (No. 1) with four independent molecules in the unit cell. The atomic coordinates are given in Table III. Figure 7 shows each molecule of the asymmetric unit and its position in the unit cell of the structure. The thiazolidine ring in each case has a C-3 conformation, assigned according to the value of the relevant torsion angle for each conformer, as predicted from the 2β-Me ^{13}C NMR chemical shift values.[17] The apparent rigidity of the fused-ring β-lactam/thiazolidine system, as evidenced by the basically identical conformation in all four molecules, is consistent with its highly strained nature. The principal differences between the four molecules lie in the orientation of the phenoxy side chain with respect to the fused bicyclic system. The five torsion angles listed in Table IV describe the side-chain conformation. Three of these are very similar for all four conformers due to intramolecular hydrogen bonding of the amide proton to the ether oxygen which results in an effective five-membered ring structure. In all cases the torsion angle C6–N14–C15–C17 is 180 ± 15°, corresponding to a planar *trans* amide bond. Further, the torsion angle N14–C15–C17–O18 is 0 ± 15°, indicating coplanarity. The angles describing torsion about the C17–O18 and the O18–C1′ bonds, however, vary widely. In Figure 8 the fused bicyclic systems of each molecular conformation have been overlayed to demonstrate the similarities in this region and the differences in the side-chain conformations.

The packing arrangement of the molecules in the lattice is one of hydrophobic layers of phenyl rings parallel to the *ab* plane,

(45) Veeman, W. S. In *Progress in Nuclear Magnetic Resonance Spectroscopy*; Emsley, J. W., Feeney, J., Sutcliffe, L. H., Eds.; Pergamon Press: Oxford, U.K., 1984; Vol. 16, pp 193–235.
(46) Duncan, T. M. *A Compilation of Chemical Shift Anisotropies*; The Farragut Press: Madison, WI, 1990; p C-32.
(47) Gall, C. M.; Cross, T. A.; DiVerdi, J. A.; Opella, S. J. *Proc. Natl. Acad. Sci. U.S.A.* **1982**, *79*, 101–105.
(48) Mehring, M. *Principles of High Resolution NMR in Solids*, 2nd ed.; Springer-Verlag: Berlin, 1983; pp 50–62. Wittebort, R. J.; Olejniczak, E. T.; Griffin, R. G. *J. Chem. Phys.* **1987**, *86*, 5411–5420.

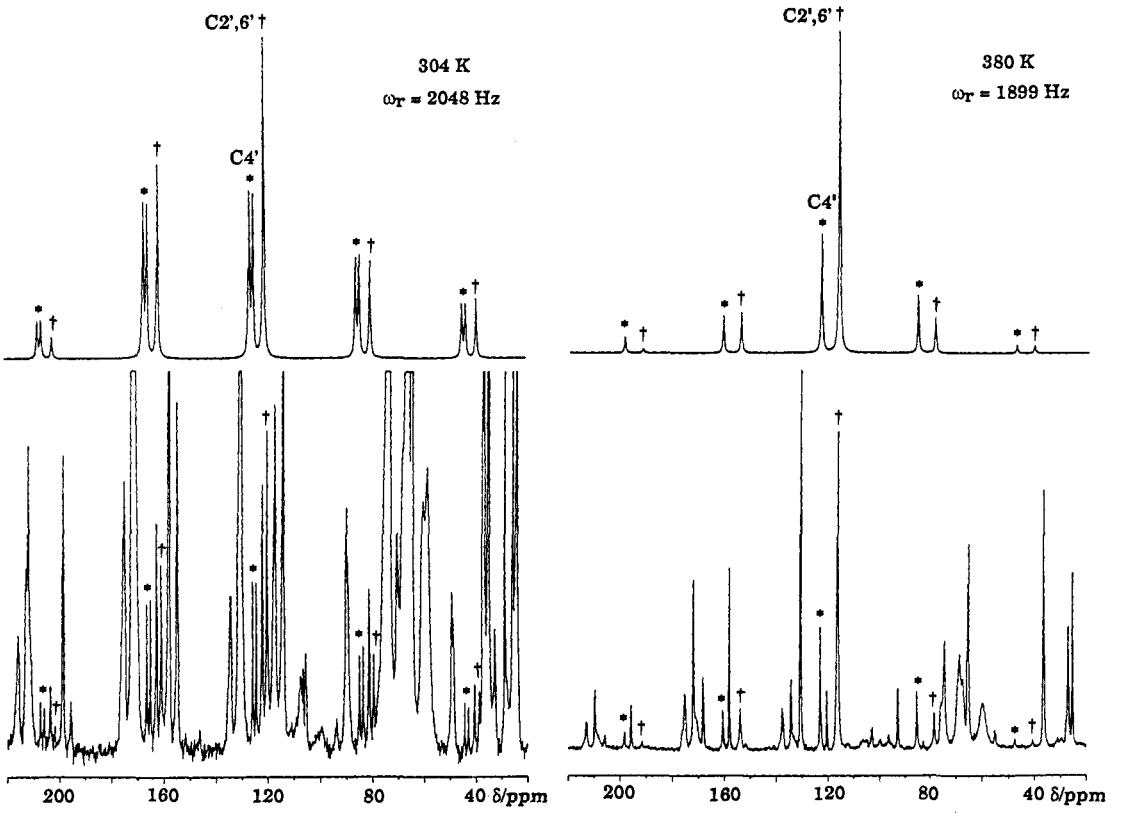

Figure 6. ^{13}C CP/MAS NMR spectra, using slow MAS rates, of potassium penicillin V at 304 and 380 K together with simulated sideband manifolds, derived from the tensors given in Table II, for the aromatic C2′,6′ and C4′ carbon sites. The isotropic peaks and the spinning sidebands of interest are marked.

Table II. Principal Values of Chemical Shift Anisotropy Tensors for Selected Aromatic Carbon Resonances in Potassium Penicillin V

site	T/K	δ_{iso}/ppm	δ_{11}/ppm	δ_{22}/ppm	δ_{33}/ppm	$\Delta\delta^a$/ppm	η
C4′	304	124.5	219	142	13	206	0.69
		126.0	218	145	15	203	0.66
	370	123.0	203	104	61	142	0.54
C2′,6′	304	120.3	178	156	26	152	0.23
	370	116.1	155	122	71	84	0.73

^{a} $\Delta\delta = (\delta_{11} - \delta_{33})$.

separated by the fused bicyclic system from hydrophilic layers of carboxylate groups and potassium ions. This arrangement provides each potassium ion with effectively seven oxygen neighbors from six penicillin V anions, two from a chelating carboxyl group, one each from two further carboxyl groups of separate molecules, two from side-chain amide oxygens of two more molecules, and the β-lactam oxygen of a sixth molecule. The local coordination polyhedra of all four independent K^+ ions in the structure are virtually identical; that for the K(1) cation is illustrated in Figure 9. Each carboxyl group makes four short contacts, two *syn* and two *anti*, to three cations, each side-chain amide oxygen has two K^+ neighbors, and each β-lactam oxygen has one K^+ neighbor. Each penicillin V anion is oriented such that four oxygen atoms face the layer of potassium ions. As a result the layers of phenyl rings have a rather open structure. This appears to be reflected in the thermal parameters for the atoms of the phenyl rings which indicate significant librations. These librations are principally in the plane of the phenyl ring for molecules **2** and **4**, but perpendicular to that plane for molecules **1** and **3**. The significance of these anisotropic parameters will be discussed further. An interesting observation concerning the packing arrangement is that although the space group symmetry is $P1$, the fused ring systems of each distinct molecule are related by a pseudo-two-fold screw axis parallel to b, with a translation of $b/4$, and the phenoxyacetamido side chains are pairwise related, **1**/**3** and **2**/**4**, by a pseudoinversion center. The structural 'frustration' that results from these different packing arrangements of the different parts of the molecular structure may explain the unusual four-fold asymmetry and the occurrence of the phase transition at higher temperature.

(b) High-Temperature Structure. For the high-temperature (373 K) diffraction data, direct methods yield a structure solution (R is ca. 17%) in which the potassium ions and penam groups have locations and orientations virtually identical to those of the low-temperature phase, but which fails to locate distinct sites for the atoms of the phenoxy side chain. From the ^{13}C CP/MAS NMR studies it was suggested that there is a dynamic disorder in the phenoxy side-chain orientation, pairwise between conformers resembling those of the ambient-temperature structure. Any conformational interchange process, although confirmed clearly as 'dynamic'[49] by NMR spectroscopy, would be slow on the time scale of the X-ray scattering phenomenon[3,50] and therefore would be detected as positional disorder with fractional occupancies for the atoms involved.

The pairwise arrangement of the four molecules in the ambient-temperature structure is apparent in Figure 7. This shows that molecules **1** and **2** have a compact conformation with their phenoxy groups on the same side of the side chain as the penam group, whereas molecules **3** and **4** have more extended conformations with the phenoxy and penam groups on opposite sides of the side chain. It was therefore proposed as an initial structure extension that the NMR observations must reflect pairwise interconversion of conformers **1** ⇌ **2** at one molecular position of the high-temperature phase and of conformers **3** ⇌ **4** at the other. This model thereby accounts for the essentially halved b-axis in the high-temperature form. Therefore the relevant pairs of molecules from the room-temperature structure were superimposed to give two possible sets of coordinates for atoms of the side chain, with

(49) Parsonage, N. G.; Staveley, L. A. K. *Disorder in Crystals*; Clarendon Press: Oxford, U.K., 1978.
(50) Dunitz, J. D.; Maverick, E. F.; Trueblood, K. N. *Angew. Chem., Int. Ed. Engl.* **1988**, *27*, 880–895.

Table III. Fractional Atomic Coordinates for Potassium Penicillin V at 293K

atom	x/a	y/b	z/c	U(iso)	atom	x/a	y/b	z/c	U(iso)
K1	0.0439(1)	0.4681(1)	0.0077(1)	0.0407	K3	0.8348(1)	0.7118(1)	-0.0085(1)	0.0392
K2	0.0357(1)	-0.0370(1)	0.0003(1)	0.0403	K4	0.8378(1)	0.2165(1)	0.0004(1)	0.0398
				Molecule 1					
S101	0.2432(2)	0.3706(1)	0.7349(1)	0.0409	C105	0.0838(5)	0.2146(4)	0.8793(3)	0.0345
N101	0.3174(4)	0.3132(3)	0.8961(3)	0.0359	C106	0.3062(5)	0.4115(3)	0.8488(3)	0.0335
N102	0.5622(4)	0.4350(3)	0.8163(3)	0.0374	C107	0.4716(5)	0.4322(4)	0.8834(3)	0.0389
O101	0.0198(4)	0.3011(3)	0.8882(3)	0.0428	C108	0.4640(5)	0.3215(4)	0.9202(3)	0.0394
O102	0.0380(4)	0.1217(3)	0.8893(3)	0.0461	C109	0.7044(5)	0.4625(4)	0.8382(3)	0.0394
O103	0.5509(4)	0.2604(4)	0.9537(3)	0.0572	C110	0.7904(5)	0.4486(5)	0.7647(4)	0.0453
O104	0.7578(4)	0.4921(4)	0.9133(3)	0.0521	C111	0.7662(6)	0.3564(6)	0.6205(4)	0.0550
O105	0.7005(5)	0.4062(5)	0.6866(3)	0.0688	C112	0.8764(7)	0.4059(6)	0.5878(5)	0.0624
C101	0.2355(5)	0.2263(4)	0.7520(3)	0.0391	C113	0.9316(9)	0.3569(7)	0.5184(5)	0.0722
C102	0.0969(7)	0.1774(5)	0.6957(3)	0.0502	C114	0.8783(9)	0.2646(8)	0.4795(5)	0.0813
C103	0.3692(7)	0.1710(5)	0.7251(4)	0.0531	C115	0.767(1)	0.2114(8)	0.5128(7)	0.0912
C104	0.2356(5)	0.2202(4)	0.8538(3)	0.0350	C116	0.7130(9)	0.2582(9)	0.5833(6)	0.0882
				Molecule 2					
S201	0.2414(2)	0.8700(1)	0.7297(1)	0.0417	C205	0.0805(5)	0.7122(4)	0.8698(3)	0.0359
N201	0.3135(4)	0.8110(3)	0.8905(3)	0.0359	C206	0.3021(5)	0.9098(3)	0.8443(3)	0.0341
N202	0.5571(4)	0.9431(3)	0.8120(3)	0.0376	C207	0.4663(5)	0.9315(4)	0.8789(3)	0.0384
O201	0.0124(4)	0.7974(3)	0.8738(3)	0.0447	C208	0.4617(5)	0.8188(5)	0.9128(4)	0.0408
O202	0.0374(4)	0.6196(3)	0.8825(3)	0.0449	C209	0.6935(5)	0.9794(5)	0.8348(4)	0.0427
O203	0.5481(4)	0.7563(4)	0.9444(3)	0.0541	C210	0.7772(7)	0.9955(6)	0.7600(4)	0.0599
O204	0.7496(5)	0.9999(5)	0.9111(3)	0.0612	C211	0.6674(7)	0.8839(5)	0.6306(5)	0.0566
O205	0.6898(5)	0.9836(4)	0.6742(3)	0.0657	C212	0.583(1)	0.8823(8)	0.5491(5)	0.0881
C201	0.2395(5)	0.7251(4)	0.7457(3)	0.0371	C213	0.553(1)	0.786(1)	0.4983(7)	0.1075
C202	0.1088(6)	0.6714(5)	0.6869(4)	0.0500	C214	0.614(1)	0.6925(8)	0.5299(7)	0.0939
C203	0.3783(6)	0.6751(5)	0.7232(4)	0.0508	C215	0.6948(9)	0.6962(7)	0.6108(7)	0.0826
C204	0.2345(5)	0.7184(4)	0.8468(3)	0.0343	C216	0.7260(7)	0.7916(6)	0.6655(5)	0.0672
				Molecule 3					
S301	0.6307(2)	0.6638(1)	0.2706(1)	0.0428	C305	0.8031(5)	0.4871(4)	0.1266(4)	0.0354
N301	0.5654(4)	0.5744(3)	0.1091(3)	0.0355	C306	0.5725(5)	0.6822(4)	0.1524(4)	0.0363
N302	0.3141(4)	0.7165(4)	0.1811(3)	0.0381	C307	0.4081(5)	0.6930(4)	0.1168(3)	0.0403
O301	0.8538(5)	0.3941(3)	0.1175(3)	0.0481	C308	0.4175(5)	0.5742(5)	0.0867(4)	0.0413
O302	0.8653(4)	0.5740(3)	0.1173(3)	0.0428	C309	0.1768(5)	0.7501(4)	0.1533(4)	0.0393
O303	0.3331(4)	0.5029(4)	0.0576(4)	0.0570	C310	0.0894(7)	0.7762(6)	0.2275(4)	0.0591
O304	0.1262(4)	0.7576(5)	0.0768(3)	0.0571	C311	0.1239(6)	0.8325(5)	0.3784(4)	0.0552
O305	0.1796(5)	0.7788(5)	0.3106(3)	0.0644	C312	0.0204(8)	0.7842(6)	0.4161(6)	0.0736
C301	0.6517(5)	0.5171(4)	0.2534(4)	0.0424	C313	-0.035(1)	0.8369(8)	0.4872(6)	0.0810
C302	0.7919(8)	0.4874(5)	0.3108(4)	0.0597	C314	0.013(1)	0.936(1)	0.5170(6)	0.0903
C303	0.5229(8)	0.4613(5)	0.2818(5)	0.0585	C315	0.116(1)	0.981(1)	0.480(1)	0.1196
C304	0.6535(5)	0.4928(3)	0.1527(3)	0.0333	C316	0.172(1)	0.9343(9)	0.4079(9)	0.1027
				Molecule 4					
S401	0.6359(2)	0.1593(1)	0.2683(1)	0.0415	C405	0.7888(5)	-0.0201(3)	0.1186(3)	0.0327
N401	0.5576(4)	0.0787(3)	0.1054(3)	0.0335	C406	0.5714(5)	0.1836(4)	0.1531(3)	0.0353
N402	0.3164(4)	0.2120(4)	0.1878(3)	0.0400	C407	0.4054(5)	0.2012(4)	0.1200(3)	0.0385
O401	0.8583(4)	0.0639(3)	0.1135(3)	0.0444	C408	0.4105(5)	0.0839(4)	0.0827(3)	0.0400
O402	0.8287(4)	-0.1153(3)	0.1034(3)	0.0452	C409	0.1713(5)	0.2301(5)	0.1642(4)	0.0453
O403	0.3230(4)	0.0171(4)	0.0492(3)	0.0554	C410	0.0828(6)	0.2246(5)	0.2377(4)	0.0548
O404	0.1179(4)	0.2460(5)	0.0896(3)	0.0598	C411	0.2063(7)	0.3220(5)	0.3660(4)	0.0547
O405	0.1667(5)	0.2243(3)	0.3230(3)	0.0587	C412	0.2943(9)	0.3166(9)	0.4490(5)	0.0857
C401	0.6397(5)	0.0119(4)	0.2471(4)	0.0424	C413	0.336(1)	0.410(1)	0.4985(7)	0.1074
C402	0.7758(7)	-0.0298(5)	0.3019(4)	0.0590	C414	0.294(1)	0.506(1)	0.468(1)	0.1089
C403	0.5048(7)	-0.0364(5)	0.2741(5)	0.0588	C415	0.211(1)	0.5104(8)	0.3850(9)	0.0938
C404	0.6385(5)	-0.0093(4)	0.1452(3)	0.0360	C416	0.1701(7)	0.4173(6)	0.3353(6)	0.0697

each assigned an occupancy of 0.5. This led to an improvement in the R-factor from 0.17 to 0.12. Refinement[51] of this model converged at $R = 0.114$, $R_w = 0.128$. The final structure solution for the high-temperature form of KpenV contains two formula units in the asymmetric unit, each penicillin molecule having two partially occupied sites for the terminal $CH_2OC_6H_5$ groups. The atomic coordinates are collected in Table V. The two molecules and their arrangement in the unit cell are shown in Figure 10.

The two molecular conformations accessible on each of the two distinct lattice sites lead to four distinct conformers in total, and to a first approximation these are remarkably similar to the four molecular conformers of the ambient-temperature structure. The slight conformational differences are revealed in the superposition in Figure 11 of all eight conformers from both structures. The packing motif in the high-temperature structure is analogous to that observed at ambient temperature, the principal difference being the presence of the two fractionally occupied positions for the side chains of each of the two molecules.

The evidence from the complementary techniques of X-ray diffraction and NMR spectroscopy supports the model of the phase transition in which a molecule on one of the two lattice sites in the high-temperature structure may be dynamically interconverted between conformers representative of two of the distinct lattice sites of the ambient-temperature structure. The compact conformers may interconvert, **1** ⇌ **2**, and the extended conformers, **3** ⇌ **4**, may do so too, but compact and extended conformers may not interchange, (**1**,**2**) ⇏ (**3**,**4**), as shown schematically in Figure 12.

An observation of interest is the change in the 2α- and 2β-

(51) The majority of the structure was refined anisotropically, but the phenoxy side chains were constrained to be planar and were refined isotropically with thermal motion and shift-limiting restraints. An increased uncertainty in the positional and thermal parameters for this case in relation to the ambient-temperature structure determination is clearly evidenced by the esd's listed in Table V and is also reflected in the higher R-values of the structure solution.

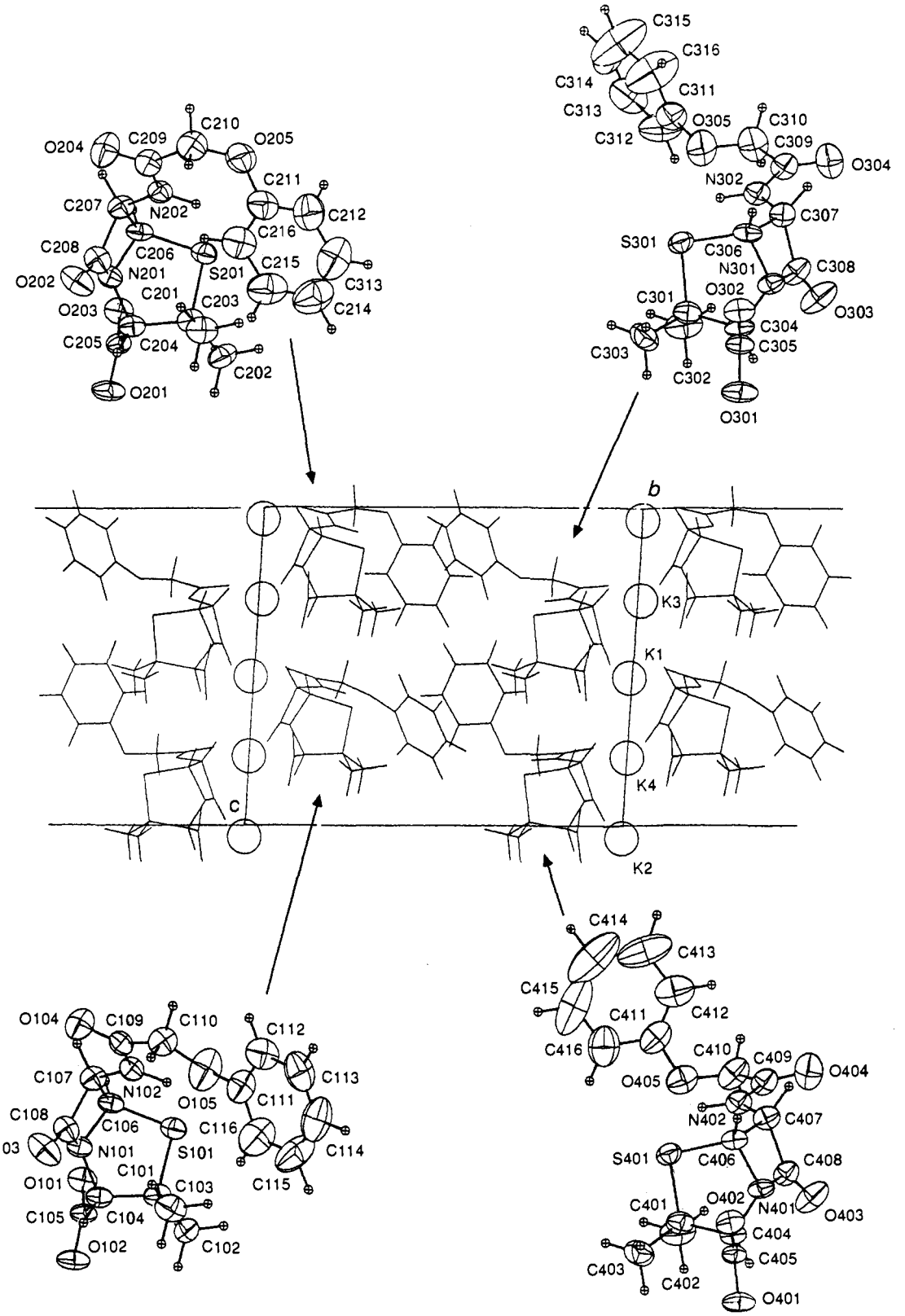

Figure 7. Ambient-temperature crystal structure of potassium penicillin V showing separately the four distinct conformers of the asymmetric unit, with 50% thermal ellipsoids, and their arrangement in the unit cell. Molecules **1** and **2** are rotated 15° about the horizontal relative to the packing diagram, and molecules **3** and **4** are similarly rotated about both the horizontal and vertical.

methyl group ^{13}C NMR chemical shifts on the phase transition, despite the lack of intramolecular conformational change in their immediate vicinity. This indicates how the methyl NMR shift is a very sensitive probe of the local environment[52] and therefore of the changes in this caused by the dynamic events involving neighboring phenoxy side chains.

(iii) Nature of the Dynamically Induced Phase Transition. The reduction in CSA of all the aromatic carbon resonances in the ^{13}C CP/MAS NMR spectrum on passing from the ambient- to the high-temperature phase is consistent with the dynamic nature

(52) Fyfe, C. A. *Solid State NMR for Chemists*; CFC Press: Guelph, Ontario, Canada, 1983.

Table IV. Torsion Angles Describing Phenoxy Side-Chain Conformations in Potassium Penicillin V Structures[a]

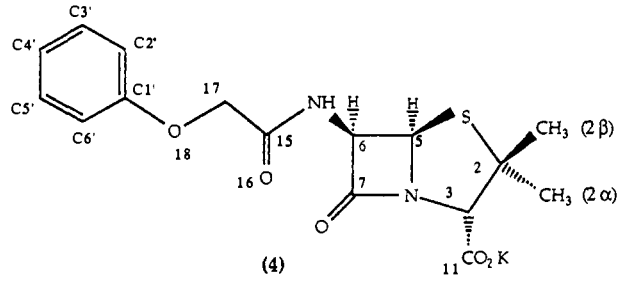

(4)

Potassium Penicillin V

angle	atom 1	2	3	4
A	C5	C6	N14	C15
B	C6	N14	C15	C17
C	N14	C15	C17	O18
D	C15	C17	O18	C1′
E	C17	O18	C1′	C2′

molecule		A/deg	B/deg	C/deg	D/deg	E/deg
293 K KpenV	1	173.6	172.3	−1.2	−160.0	−51.5
	2	168.7	−176.2	8.4	−86.7	−179.6
	3	165.5	−178.0	11.0	161.0	77.3
	4	178.5	171.6	12.8	87.0	−177.6
373 K KpenV	1	171.3	167.6	6.0	−160.1	−62.8
	2	171.3	−177.5	20.0	−101.7	−168.1
	3	170.7	−164.9	−10.0	168.5	76.9
	4	170.7	173.8	−0.5	93.9	−174.3

[a] A positive rotation is anticlockwise from atom 1 when viewed from atom 3 to atom 2.

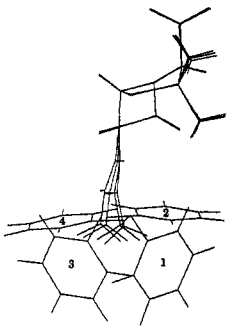

Figure 8. Superposition of the four distinct molecular conformers found in the ambient-temperature structure of potassium penicillin V. Note the almost identical conformations of the fused β-lactam/thiazolidine ring system in each case and the large differences in the phenoxy ring orientation between conformers. These differences are defined in terms of the relevant torsion angles in Table IV.

of the disorder. The solution of the high-temperature structure enables this to be verified quantitatively by calculation of the expected change in the CSA of the C4′ resonance on interconversion between the half-occupied sites detected in the crystallographic studies at a rate rapid on the CSA time scale ($>\approx 10^4$ s^{-1}).

Chemical shift tensors were determined at 304 K for the two C4′ resonances that each account for a single distinct site. These peaks have almost identical CSAs (Table II), and it was assumed that this is likely to be the case for all the distinct molecules in the structure. In the high-temperature form only a single center band, representing the accidental degeneracy of the C4′ aromatic resonances of the two crystallographically independent molecules in this phase, was observed. This combined sideband manifold was fitted to a single tensor interaction (Table II), although strictly the sideband manifold intensities should be simulated as a superposition of two independent and equal contributions from the two distinct carbon atom types this represents.

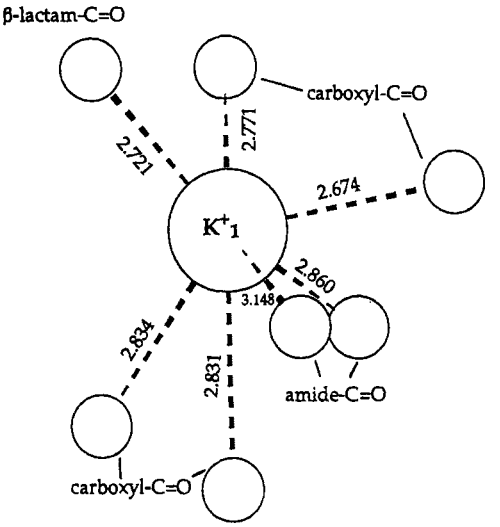

Figure 9. Local coordination sphere of oxygen atoms around the K1 ion in the ambient-temperature crystal structure of potassium penicillin V. A similar arrangement is found for all the four distinct potassium ions in the structure.

The extent of the conformational interchange process on the static CSA may be determined using order parameter theory and an estimate of the magnitude and orientation of the static CSA tensors appropriate to the sites involved in the dynamic averaging. Assuming the model orientation of the static tensors with respect to the phenyl ring,[45] rotation matrices describing each of the two independent side-chain interconversion processes[53] were determined from the crystallographic coordinates for the two half-occupied sites within each conformer pair. The rotation matrices and their corresponding Euler angle formulations are given in Figure 13. Assuming that all orientations in the high-temperature phase have anisotropies and asymmetries for the static CSA tensor of the C4′ carbon atoms identical to those measured in the ambient-temperature phase, the averaged CSA tensors expected on the basis of the crystallographic structure were calculated and are presented in Table VI. For a direct comparison with experiment the sideband manifolds expected at an MAS rate of 1899 Hz were simulated for each averaged C4′ tensor and their summation with equal weighting was compared with the experimental sideband profile of the combined C4′ resonance. For comparison the sideband manifolds for the calculated best single tensor fit and for the static tensor values measured at 304 K are provided. The intensities calculated on the model of dynamic disorder fit the observed manifold well; the small differences between the measured and calculated sideband manifolds are likely to be due to the increased libration of the phenyl ring carbons in the high-temperature form, which is evident from inspection of the thermal parameters. These vibrational motions will average the CSA such that the quasistatic tensors necessary for the calculation will be averaged somewhat in comparison to those of a truly static aromatic ring. This calculation confirms that the conformational interconversion event detected by CP/MAS NMR does indeed correspond to the side-chain disorder present in the high-temperature X-ray crystal structure solution.

Conclusions

The ambient-temperature form of KpenV adopts an elaborate structure with four molecules in the asymmetric unit. It is interesting to speculate as to the reasons for this. From combined solid-state NMR and single-crystal diffraction studies, we have determined[54] that RbpenV is essentially isostructural

(53) Only the reorientational and not the translational component of each trajectory is important for determination of second-rank tensor averaging.

(54) Wendeler, M.; Fattah, J.; Edwards, A. J.; Prout, C. K.; Dobson, C. M.; Heyes, S. J. American Crystallographic Association Meeting, Pittsburgh, 1992.

Table V Fractional Atomic Coordinates for Potassium Penicillin V at 373K

atom	*x/a*	*y/2b*	*z/c*	*U*(iso)
K1	1.0393(6)	0.9727(4)	0.0034(4)	0.0571
K2	0.8349(6)	0.7218(4)	−0.0045(4)	0.0578
		Molecule 1		
S101	0.2432(6)	0.3711(5)	0.7353(4)	0.0587
O101	0.015(1)	0.3050(9)	0.8841(7)	0.0639
O102	0.038(1)	0.1278(9)	0.8896(8)	0.0697
O103	0.547(1)	0.262(1)	0.9518(9)	0.0788
O104	0.750(1)	0.503(1)	0.9119(8)	0.0743
O105	0.688(2)	0.412(2)	0.688(1)	0.087(5)
O205	0.689(2)	0.488(1)	0.683(1)	0.082(5)
N101	0.316(1)	0.3160(9)	0.8949(7)	0.0498
N102	0.560(1)	0.4401(9)	0.8173(7)	0.0545
C101	0.238(1)	0.227(1)	0.7538(8)	0.0533
C102	0.101(2)	0.179(1)	0.696(1)	0.0744
C103	0.374(2)	0.172(1)	0.730(1)	0.0724
C104	0.235(1)	0.2236(9)	0.8536(8)	0.0486
C105	0.084(1)	0.217(1)	0.8788(7)	0.0490
C106	0.305(1)	0.413(1)	0.8493(8)	0.0534
C107	0.471(1)	0.434(1)	0.8833(8)	0.0535
C108	0.460(1)	0.325(1)	0.9165(8)	0.0552
C109	0.696(1)	0.471(1)	0.8396(9)	0.0609
C110	0.783(2)	0.449(3)	0.763(2)	0.090(6)
C111	0.767(1)	0.357(1)	0.6265(9)	0.092(5)
C112	0.870(1)	0.413(1)	0.591(1)	0.095(6)
C113	0.921(1)	0.370(2)	0.517(1)	0.104(7)
C114	0.870(2)	0.271(2)	0.477(1)	0.110(7)
C115	0.768(2)	0.215(1)	0.512(1)	0.103(7)
C116	0.718(1)	0.257(1)	0.587(1)	0.102(7)
C210	0.785(2)	0.480(2)	0.764(2)	0.080(6)
C211	0.676(1)	0.387(1)	0.633(1)	0.104(6)
C212	0.611(1)	0.381(2)	0.546(1)	0.120(8)
C213	0.591(1)	0.283(2)	0.497(1)	0.134(8)
C214	0.638(2)	0.190(2)	0.537(2)	0.133(9)
C215	0.704(2)	0.196(2)	0.624(2)	0.128(8)
C216	0.723(1)	0.295(2)	0.672(1)	0.119(8)
		Molecule 3		
S301	0.6302(6)	0.1713(5)	0.2672(4)	0.0599
O301	0.856(1)	0.0766(8)	0.1135(7)	0.0633
O302	0.838(1)	−0.099(1)	0.1091(8)	0.0762
O303	0.324(1)	0.019(1)	0.0531(8)	0.0703
O304	0.122(1)	0.265(1)	0.0854(7)	0.0762
O305	0.181(2)	0.283(2)	0.311(1)	0.076(5)
O405	0.153(2)	0.233(1)	0.314(1)	0.071(3)
N301	0.558(1)	0.0845(9)	0.1077(7)	0.0516
N302	0.312(1)	0.224(1)	0.1838(7)	0.0589
C301	0.644(1)	0.025(1)	0.2497(8)	0.0617
C302	0.783(2)	−0.008(2)	0.304(1)	0.0846
C303	0.517(2)	−0.030(2)	0.276(1)	0.0886
C304	0.643(1)	0.0013(9)	0.1493(8)	0.0508
C305	0.792(1)	−0.008(1)	0.1215(8)	0.0572
C306	0.569(1)	0.192(1)	0.1543(8)	0.0541
C307	0.405(1)	0.205(1)	0.1191(8)	0.0574
C308	0.412(1)	0.086(1)	0.0855(9)	0.0604
C309	0.174(1)	0.250(1)	0.1592(9)	0.0630
C310	0.097(3)	0.295(4)	0.230(2)	0.086(6)
C311	0.123(2)	0.343(1)	0.378(1)	0.097(7)
C312	0.001(2)	0.305(1)	0.408(2)	0.108(8)
C313	−0.038(2)	0.349(2)	0.486(2)	0.121(9)
C314	0.045(3)	0.431(2)	0.535(1)	0.124(9)
C315	0.167(3)	0.468(1)	0.506(1)	0.125(9)
C316	0.206(2)	0.425(1)	0.428(2)	0.115(8)
C410	0.073(1)	0.259(2)	0.230(1)	0.080(5)
C411	0.210(1)	0.330(1)	0.3654(9)	0.101(5)
C412	0.301(1)	0.323(2)	0.4446(9)	0.119(7)
C413	0.347(1)	0.415(2)	0.498(1)	0.132(8)
C414	0.303(2)	0.515(2)	0.471(1)	0.129(8)
C415	0.211(2)	0.522(1)	0.392(1)	0.128(8)
C416	0.165(1)	0.430(1)	0.339(1)	0.114(7)

with KpenV but that H-, Na-, and CspenV have structures with a single molecule in the asymmetric unit and that LipenV has a structure with two molecules in the asymmetric unit. The molecular packing in the structures of penicillin V salts appears to be dictated by the size of the cation and its coordination requirements, and this must be an important criterion that leads to only the potassium and rubidium salts adopting the complex structure. This will be addressed in a forthcoming paper.[55] Of importance is the observation of the pseudosymmetry elements in the structure. It is a well-known principle that molecular solids will always attempt to adopt structures with the highest symmetry possible.[56] We observe that the rigid fused bicyclic units of each distinct molecule are of essentially identical intramolecular conformation and, when isolated in the structure, are related by a pseudoscrew axis. The phenoxy side chains show variability at two of their torsion angles, and when the side chains are considered in isolation, they may be regarded as being pairwise related through inversion symmetry. The four-fold asymmetry of the overall structure appears to arise as a result of an incompatability between the packing motifs of the two parts of the molecule. Interestingly, it is the existence of this low-symmetry unit cell with four distinct molecular conformers which provides the opportunity to probe in such detail the molecular structure and dynamics of this system.

The NMR spectra reveal that the aromatic rings of the penicillin V molecules are undergoing 180° flips about their two-fold axes. This motion is not apparent from the X-ray diffraction structure, because it does not give rise to positional disorder. It is, however, detected by the NMR experiments, because of motional averaging effects. This is an example of the complementarity of NMR and X-ray diffraction techniques, because of their very different characteristic time scales. Examination of the X-ray structure suggests that fluctuations in neighboring molecules relative to the equilibrium atomic positions are required in order for such ring flips to occur. This is a general observation in most systems, since looser packing in the region of the phenyl rings results generally in effectively diffusive disorder of the ring position about its two-fold axis. The presence of four distinct molecules in the asymmetric unit of the ambient-temperature structure provides the opportunity to question whether the individual 180° flips of the aromatic rings are correlated in any manner. The aromatic rings may be considered as forming a stack motif in a plane running through the structure, not dissimilar from motifs which have received attention with regard to models for calculations of aromatic ring flip processes in glassy polycarbonate.[57] The conclusion of those studies is that at least some aspects of the ring motion are cooperative but that the ring flips of neighboring rings need not be concerted. If this were the case for KpenV, it might be expected that the ring flip rates of molecules **1** and **2**, and similarly those of molecules **3** and **4**, should be correlated. From the NMR spectra the rings of the distinct molecules appear to have different characteristic flip rates at any given temperature, and the ring flips in KpenV are therefore assumed to be uncorrelated. Evidently, neighboring rings are not required to flip in a cooperative manner to enable a ring to flip. This evidence mitigates against a concerted mechanism and argues for a scenario in which ring flips are "nonequilibrium" events, occurring only when the local environment of the ring is distorted significantly from its equilibrium position, as has been suggested from molecular dynamics simulations of proteins.[58] Ring flips may be regarded as 'rare' events. The actual ring flip event may only last on the order of 10^{-12}–10^{-15} s, and at a frequency of flipping of 10^{6} s^{-1}, this implies that no significant electron density will be detected away from the equilibrium atomic positions in the X-ray diffraction study. The crystal structure solution is therefore not

(55) Wendeler, M.; Fattah, J.; Edwards, A. J.; Prout, C. K.; Dobson, C. M.; Heyes, S. J. Unpublished results.

(56) Kitaigorodskii, A. I. *Molecular Crystals and Molecules*; Academic *Press*: New York, 1973.

(57) Schaefer, J.; Stejskal, E. O.; Perchak, D.; Skolnick, J.; Yaris, R. *Macromolecules* **1985**, *18*, 368–373. Romiszowski, P.; Yaris, R. *J. Chem. Phys.* **1991**, *95*, 6738–6744.

(58) McCammon, J. A.; Lee, C. Y.; Northrup, S. H. *J. Am. Chem. Soc.* **1983**, *105*, 2232–2237. Karplus, M.; McCammon, J. A. *Annu. Rev. Biochem.* **1983**, *53*, 262–300. Northrup, S. H.; Pear, M. R.; Lee, C.; McCammon, J. A.; Karplus, M. *Proc. Natl. Acad. Sci. U.S.A.* **1982**, *79*, 4035–4039.

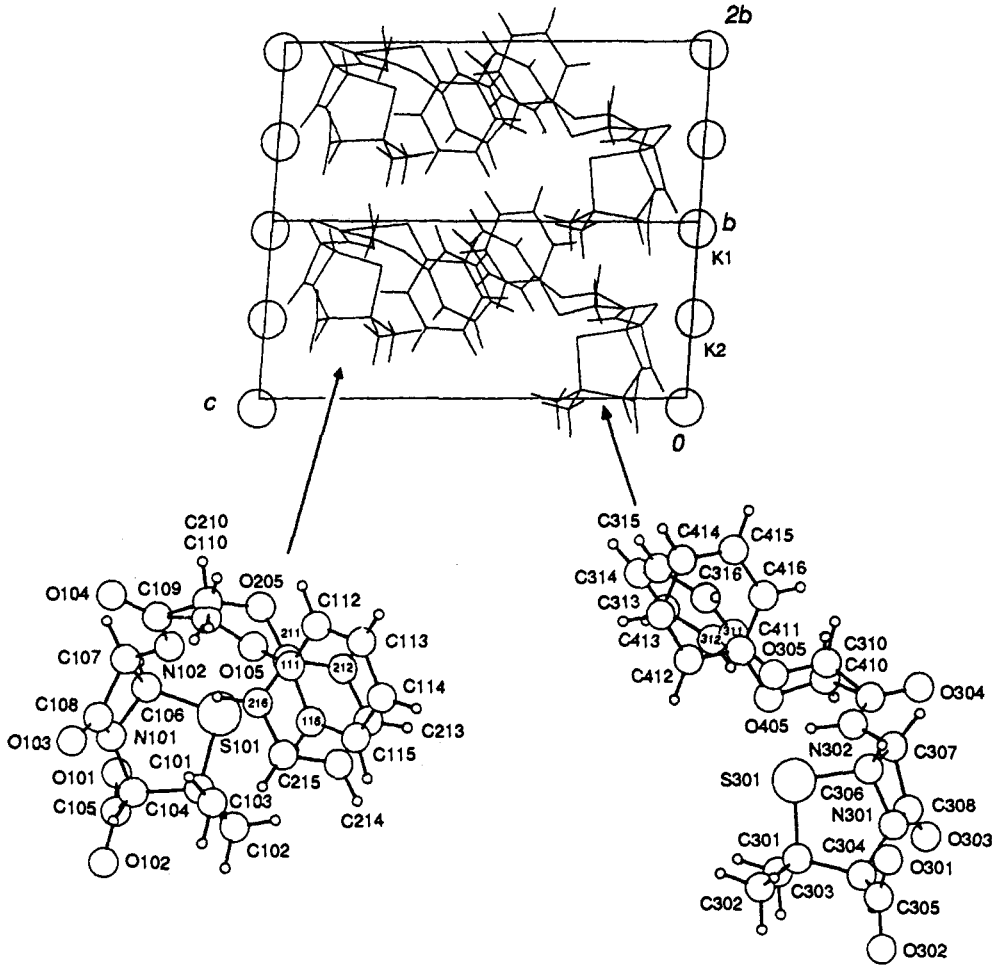

Figure 10. High-temperature (373 K) crystal structure of potassium penicillin V, showing separately the conformers present in the asymmetric unit, with isotropic temperature factors, and also their arrangement in the unit cell.

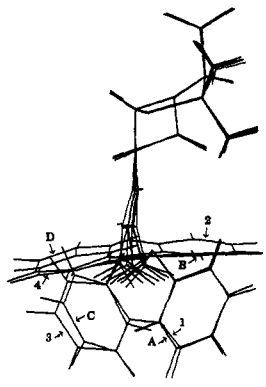

Figure 11. Superposition of the conformers present in the ambient- and high-temperature crystalline phases of potassium penicillin V. Eight conformers can be distinguished in four separate pairs. The conformers of the ambient-temperature structure are labeled 1–4, and those of the high-temperature structure, A–D (A and B are the conformers of crystallographic molecule **1**, and C and D, the conformers of molecule **3**).

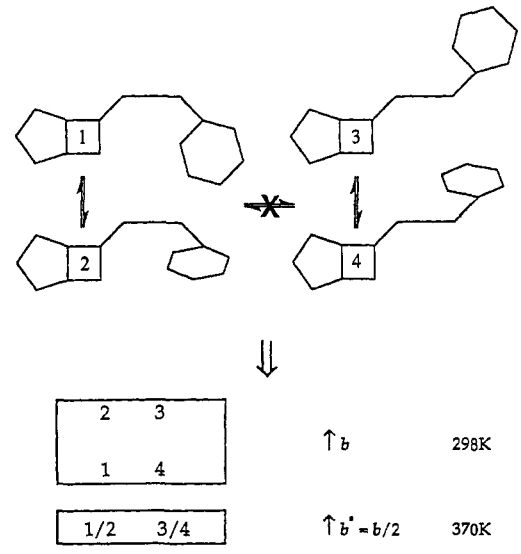

Figure 12. Schematic illustration of the pairwise conformational interconversion process and the manner in which it leads to the observed phase change.

incompatible with the "nonequilibrium" distortion mechanism for the ring flip.

The detection of aromatic ring flips was one of the first direct observations of specific dynamical events in the interior of proteins.[13] That similar events occur in molecular crystals is therefore of interest in efforts to understand the dynamics of protein molecules. In this respect the penicillins are likely to be particularly valuable because they are derivatives of tripeptides; the intermolecular interactions within the crystals therefore involve forces similar to those in the interior of proteins. The regular repetitive packing motif that determines the local structural environment in the penicillins is different from that generated by the secondary structure of proteins, which is determined by the continuous polypeptide chain. Nevertheless, the fact that similar dynamic behavior occurs in both these 'close-packed' environments suggests that the dynamics of crystalline penicillins may be regarded as a simple, but interesting, model for side-chain motions

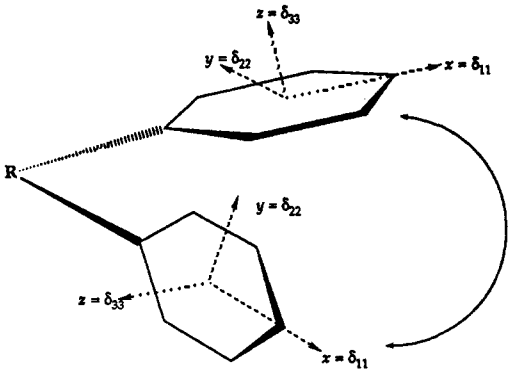

-0.697086	-0.345630	-0.628181
-0.710608	0.216440	0.669467
-0.095426	0.913062	-0.396487

Rotation matrix for 1 / 2 pair of molecules (molecule 1 at high temperature)

θ = 113.4°
φ = 46.8°
ψ = 84.0°

-0.687966	0.180926	0.702830
-0.711665	0.0216525	-0.702181
-0.142259	-0.983262	0.113869

Rotation matrix for 3 / 4 pair of molecules (molecule 3 at high temperature)

θ = 83.5°
φ = -45.0°
ψ = -81.8°

Figure 13. Schematic illustration of the pairwise dynamic intramolecular interconversion processes for the phenoxy side chain of potassium penicillin V in the high-temperature crystalline phase, for each of the two molecules of the crystallographic asymmetric unit. The rotation matrices and Euler angles for each interconversion process are given.

Table VI. Experimentally and Theoretically Derived Chemical Shift Tensor Components for the C4′ Aromatic Site at 370 K in KpenV

origin of tensor	δ_{11}/ ppm	δ_{22}/ ppm	δ_{33}/ ppm	$\Delta\delta$	η
mean principal component values of NMR-calculated static tensor after averaging through rotation matrix 1	219	144	14	205	0.67
matrix 1	204	116	57	147	0.75
matrix 2	202	100	75	127	0.33
observed fit to a single tensor	203	104	61	142	0.54

Sideband Manifold Intensities for a MAS Rate of 1899 Hz

	sideband order				
	2	1	0	−1	−2
intensity average from matrix 1	0.13	0.37	1.0	0.47	0.08
average from matrix 2	0.12	0.25	1.0	0.43	0.04
$^1/_2$(matrix 1) + $^1/_2$(matrix 2)	0.13	0.32	1.0	0.45	0.06
experimental	0.14	0.32	1.0	0.47	0.09
single tensor fit	0.14	0.32	1.0	0.49	0.11
304 K 'static' tensor	0.33	1.13	1.0	0.71	0.43

in proteins. It is therefore of considerable significance that a large-scale motion of the side chain of KpenV has been detected here, as it may be related to side-chain motions thought to occur for some residues in proteins.[59] Furthermore, the side-chain interconversion of KpenV appears to be closely related to side-chain motions detected in the homopolymer poly(γ-benzyl-L-glutamate) by ^{2}H NMR.[60] The packing of the penam groups appears essentially undisturbed by the phase transition associated with the side-chain motion of KpenV and in this manner resembles a rigid backbone, reinforcing the analogy with macromolecular systems formed from equivalent repeating units. The dynamics occurring in small molecular crystals like KpenV can be studied in much more detail than can those in the more complex macromolecular systems, and further experimental and theoretical work should give increased insight into their origin and significance. Studies of the type detailed here may perhaps 'bridge' work on small and large molecular systems, in addition to contrasting the behavior of small molecules in crystalline and solution states.

An important question arising from the present study concerns the manner in which the ambient- and high-temperature structures of KpenV are related through the order/disorder phase change. The calculated densities of the ambient- and high-temperature phases, at 1.49 and 1.43 g cm^{-3}, respectively, are within the normal range for similar close-packed molecular crystals and indicate only slight expansion of the structure through the phase transition. The high-temperature structure appears to involve large-angle interchanges between conformers present in an ordered fashion in the ambient-temperature form. Within experimental error the penam units are arranged in precisely the same manner as in the ambient-temperature structure, and the side chains at each molecular position are disordered dynamically between two conformations of the ambient-temperature structure that are unrelated by the pseudoinversion center. A pseudoinversion center still relates the partially occupied side-chain conformations of the two distinct molecules of the structure. The phase transition and the conformational interchange are likely to be driven by entropic factors, made possible by the variability inherent in the torsion angles determining the side-chain conformation. It is interesting that the magnitude of the conformational interconversions observed shows that large fluctuations are possible, even in crystals. Although the interconversion observed can be described justifiably as a "large-angle" change, it is intriguing to note that the conformers related by the pseudoinversion symmetry cannot interconvert. From inspection of the ambient- and high-temperature structures in Figures 7 and 10 and the schematic Figure 12, it is apparent that this interconversion would involve considerably greater disruption of the crystal packing than the motions that are observed to occur at these temperatures.

The diffraction studies reveal the intricacies of the limiting structures involved in the crystalline transition, but questions remain concerning the intimate mechanism of the phase change. There is some evidence from the NMR spectra in the region of the structural transition that the spectra are not a simple superposition of the resonances characteristic of the two pure phases involved in the conversion. This suggests some modification of the parent structures within the transition regime. Considering the proportion of molecules at the phase boundary to be negligible, the spectra expected from a classical nucleation and growth mechanism will be superpositions of those of the characteristic ordered phases.[61] We suggest that the changes could occur initially in a macroscopically continuous and microscopically homogeneous manner, such that, on heating the ambient temperature phase, conformationally disordered molecules begin to occur randomly, but with increasing probability as the temperature increases. The NMR spectrum of any molecule is expected to depend upon its local environment, in addition to its intramolecular conformational properties. In a homogeneous change, the local environments of the molecules will change progressively as the transition proceeds and so the spectra of ordered and disordered molecules will be modified from their appearance in the pure phase. We assume that eventually the number of molecules of the new phase must exceed the solubility limit in the old phase, phase separation will occur, and a discontinuous transition will be detected. The transition will complete via growth at the phase boundary in the normal manner.[62]

(59) Dobson, C. M.; Karplus, M. *Methods Enzymol.* **1986**, *131*, 362–389. Smith, L. J.; Sutcliffe, M. J.; Redfield, C.; Dobson, C. M. *Biochemistry* **1991**, *30*, 986–996.

(60) Meirovitch, E.; Samulski, E. T.; Leed, A.; Scheraga, H. A.; Rananavare, S.; Némethy, G.; Freed, J. H. *J. Phys. Chem.* **1987**, *91*, 4840–4851.

(61) Rigamonti, A. *Adv. Phys.* **1984**, *33*, 115–191. Heyes, S. J. D.Phil Thesis, University of Oxford, U.K., 1989.

(62) Rao, C. N. R.; Rao, K. J. *Phase Transitions in Solids*; McGraw-Hill: New York, 1977.

In this study the combined approach of NMR spectroscopy and single-crystal X-ray diffraction has shown a synergy, whereby input on structural constraints and information concerning dynamics from NMR spectroscopy have facilitated structure solution from X-ray diffraction data. Furthermore, the detailed structural information from a successful single-crystal diffraction refinement has complemented the NMR data to allow detailed interpretation of dynamic events, not fully characterized by NMR alone. The combination of solid-state NMR and X-ray diffraction in this manner should prove an important general methodology for the study of molecular structure and dynamics. Also, this work shows how investigation of small molecules, which may be studied in detail, may help elucidate features of the structural properties of large molecules. Potassium penicillin V has proved to be a model system in which many features of the structural and dynamic complexities of molecular crystals may be investigated in unusual detail, not least because of its low-symmetry structure and its high-temperature phase change, above which molecular side-chain conformations are interchanged by a remarkable large-angle dynamic process.

Acknowledgment. We thank M. J. Seaman for the tensor-averaging computer program, Dr. J. Everett and A. E. Bird for some samples of KpenV, and Prof. D. C. Hodgkin and Dr. D. P. Raleigh for useful discussions. We also wish to thank M. Odlyha for performing the DSC measurements and Drs. A. M. Glazer and F. Wondre for the variable-temperature X-ray powder diffraction. J.M.T. thanks the EPA Cephalosporin and Educational Trusts and Pembroke College for financial assistance. S.J.H. thanks the Glasstone Benefaction for a Fellowship. The SERC is thanked for financial support.

Supplementary Material Available: Tables of room-temperature and high-temperature determinations of atomic coordinates, thermal parameters, bond distances and angles, and interionic contact distances and tables of crystallographic data (33 pages); tables of room-temperature and high-temperature structure factors (57 pages). Ordering information is available on any current masthead page.